

Corrosion of Glass Windows in DIRC PMTs

P. Bourgeois and J. Va'vra

Stanford Linear Accelerator Center, Stanford University, Stanford, CA 94309

Work supported by Department of Energy contract DE-AC03-76SF00515.

Corrosion of Glass Windows in DIRC PMTs

P. Bourgeois and J. Va'vra

Abstract

The DIRC photon detector contains ~11,000 photomultipliers (PMTs), which are submerged in ultra-pure water. This note reports on glass corrosion R&D conducted with PMTs in pure water. We conclude that only limited number (~50) of the PMTs in water are affected by rapid corrosion, while a majority of the 11,000 PMTs should last, according to our measurements, for another ten years. The observation of PMT glass corrosion is based on visual observations, X-ray surface analysis, ESCA surface analysis, weight analysis, transmission measurement, as well as detailed water trace element analysis. We also correlate these observations with DIRC measurements of water pH factor, resistivity, temperature, transmission, and BaBar analysis of Bhabha and di-muon events. We also compare DIRC water purity with that of the Super Kamiokande and K2K experiments, which also use ultra-pure water. We provide empirical proof that corrosion, in our particular Borosilicate type of PMT glass window, occurs at high rate when the glass has no Zn content.

1. Introduction

DIRC is using EMI 9125FLB17 1.125" diameter. PMTs made by Electron Tube Ltd. (ETL). The PMT front glass window is made of B53 Borosilicate glass (also called E53C). B53 is specified as a low background glass because it has no potassium (K). One should also add that the front glass is different than the side glass (see Section 6). There is ~11,000 PMTs of this type in the photon detector. The PMT front windows are sitting in water to minimize photon losses. The front window is only 1.2 ± 0.1 mm thick. The window type and its thickness were chosen to maximize a response at very low wavelengths. In retrospect, DIRC could have used a thicker window because the EPOTEK-301-2 optical epoxy, used to glue quartz bars together, cuts the wavelength acceptance below 290 nm. However, that was not initially realized.

In principle, ultra-pure water is very corrosive because it is hungry for ions. This creates a certain electrostatic pressure pushing a migration of ions from any surface surrounding water. Therefore, when designing an experiment in such water, one has to worry about corrosion of all components, including the vessel (in DIRC we call it the SOB, for stand-off-box), plumbing, and glass windows of PMTs. The pure water is required in an experiment such as DIRC to reach good optical transmission in 1 m of length, as well as a bacteria-free environment.

Examples of experiments using a large number of PMTs submerged in ultra-pure water are the DIRC, Super Kamiokande, K2K, SNO, Sudan, Milargo, etc. Typically, the PMTs are submerged in water to minimize photon losses due to windows and couplings.

It is certainly tempting to argue at this point that there is already enough experience running glass PMTs in clean water, and therefore one does not have to worry, arguing PMT manufacturers already know. Unfortunately, this argument is incorrect. We have found that there is a relatively low level of understanding, from a theoretical point of view when questions are raised about under what condition a glass will corrode. However, since several experiments have been running for the past 3-4 years with very large number of PMTs in water, the relevant empirical experience is slowly emerging, and DIRC certainly will contribute to the data in this area. Nevertheless, we would always recommend performing exhaustive corrosion tests for particular choice of glass formulation.

When the DIRC vessel (SOB) was opened and drained in October 1999, we noticed that many of the PMTs front glass windows had a "milky" or "frosty" appearance. Figure 1 shows examples of corroded PMTs, and, for comparison, one that is clear. We found that only the glass face was corroded, i.e., the PMT sides were not affected at all. The "frosty" PMT had deep surface fractures resembling a frosty window in winter. The "milky" surface appears to be slightly cloudy, and visible only under direct light. For example, if a "milky" PMT is submerged in water, the problem is almost unnoticeable. This is because water provides good optical coupling even to corroded surfaces. A "frosty" PMT is slightly more noticeable in water. We did a visual accounting¹ of

¹ The determination of what PMT should be labeled "milky" versus "frosty", as well as locating them in the SOB, was done

*Work supported by Department of Energy contract DE-AC03-76SF00515.

all affected PMT in the entire SOB during the October shutdown, and the result is that about two-thirds of them are in the “milky” category, and the number of “frosty” PMTs is ~50. One should also point out that to date, we do not have an independent account of the number of bad PMTs, i.e., verified by the manufacturer.

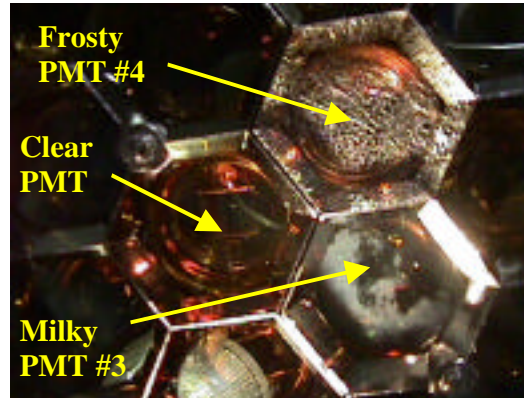


Figure 1. Example of a “milky” PMT (labeled as #3), and a “frosty” PMT (labeled as #4), observed in the SOB during October 1999, when water was drained out of the vessel.

A subsequent DIRC data analysis found no deterioration of the relative efficiency of the “milky” or “frosty” PMTs compared to “clear” PMTs, which confirms that water provides a good coupling to these surfaces. In fact, a lab test on a “frosty” PMT yielded normal results, i.e., no after-pulsing, which would indicate worsening vacuum. The long-term behavior of relative efficiency is still being investigated.

We have removed a number of “frosty” and “milky” PMTs from the SOB during the October 1999 shutdown, for subsequent surface analysis at the ETL Company, Saclay, and SLAC. We briefly outline the sequence of various major developments:

- (a) First, by using an electronic microscope at SLAC, the problem was identified as glass corrosion of the PMT front window, characterized by a depletion of sodium ions [2].
- (b) ETL confirmed this explanation by measuring the glass composition after immersion in hot water and comparing it to the nominal composition [3,4]. The measurement is done by X-ray fluorescence. The X-rays probe the surface composition to a depth between 10-100 μm . Results are given in Table 1. The surface composition of the glass has been modified as a result of immersion for 31 days at 83.5°C. In particular, the fraction of alumina, boron, and silicate (Al_2O_3 , B_2O_3 and SiO_2) constituents has increased after immersion because other constituents, and especially sodium, have been leached from the surface layer.
- (c) Most importantly, ETL discovered that the “frosty” PMTs were in fact those PMTs, which had mistakenly received a window made out of the wrong material [3,4]. The glass material had no zinc, and was identified as X-glass (or E47.2-type glass, which is used by ETL for other applications), instead of the nominal B53 glass, which is required for its better resistance to corrosion when submerged in the ultra-pure water. A subsequent test conducted at SLAC using the ESCA analysis confirmed that indeed the “frosty” PMTs had no zinc in the first 50Å below the surface [5]. Table 1, provided by the ETL Company, gives the glass composition before and after immersion of the wrong type of glass in water. For this glass, not only the sodium, but also the boron was depleted. The company found that windows made out of X-glass are already frosty after five days of being submerged in hot water at 83.5°C, which corresponds according to ETL, to about 5 months at ambient temperature, as we discuss later. This is a crucial result on which to base the argument that the SOB PMTs, made out of X-glass have already become “frosty” by the time of the October 1999 shutdown, and therefore, we count all.
- (d) Tests performed in Saclay verified the ETL scaling law of glass corrosion in B53 material. Even more

by J. Va’vra and A. Hoecker during the October 1999 shutdown [1]. Unfortunately, to this date, there is no other direct source of information on how many PMTs are affected. For example, after one year of operation the DIRC data analysis, is still unable to distinguish which are the “clear”, “milky”, or “frosty” PMTs. Similarly, the PMT manufacturer did not provide the information how many PMTs were made out of the “wrong” type of glass.

importantly, the Saclay data shows a loss of the PMT detection efficiency, which could be explained by either the window transmission degradation, the quantum efficiency loss, or gain drop. The loss of the detection efficiency may be consistent with a 2-3% loss of photons we seem to detect in DIRC data from BaBar, both in the Bhabha and the di-muon events.

(e) Many other tests from Saclay, ETL, and SLAC were performed to check for overall consistency.

Table 1. ETL Co. analysis of B53 and X-glass windows under various conditions.

Component	B53 glass ref. glass [% by wt]	B53 glass immersed for 30 days, 83.5°C	B53 glass normalized to SiO ₂ **	X-glass ref. glass	X-glass immersed for 30 days, 83.5°C	X-glass normalized to SiO ₂ **
SiO ₂	62.70	66.10	62.70	69.60	92.40	69.60
NaO ₂	7.50	1.00	0.95	8.70	0.90	0.68
Al ₂ O ₃	6.80	7.30	6.92	4.20	5.10	3.84
ZnO	2.90	2.70	2.56	0.00	0.000	0.00
BaO	3.10	2.40	2.28	0.00	0.20	0.15
CaO	0.70	0.80	0.76	0.00	0.70	0.53
B ₂ O ₃ *	15.90	19.10	18.12	17.20	0.00	0.00
Total	99.60	99.40	94.29	99.70	99.30	74.80

Notes: * Fitted by difference

** Normalized to maintain the SiO₂ composition constant.

2. Tests Performed at the Electron Tube Ltd. (ETL)

2.1. Overview

This section describes tests performed at ETL [3,4]. The goal of the study is to quantify the rate of material loss of the glass in order to answer the question of whether the PMTs could survive ten years in the DIRC SOB vessel without imploding. The study was performed in hot de-ionized water in order to accelerate their aging effect. The acceleration factors applied have been measured by a separate study.

In addition, X-ray fluorescence analysis of the immersed and non-immersed glass windows has been used to measure the composition of the glass in order to improve the understanding of the weight loss mechanisms, as already mentioned in the introduction.

2.2. Experimental Setup

2.2.1. “Thirty Day” Trial

B53 (also called E53C by ETL in these tests) glass window samples (2.93cm dia. and 0.12cm thick) were immersed in de-ionized water for 31 days at 83.5°C. The windows were positioned flat on the base of an immersed perforated polypropylene beaker to enable the whole surface area of the window to be exposed to attack by water. The de-ionized water was changed daily. First, water in system A was replaced with fresh de-ionized water from our in house supply. Then the water in system B was replaced with water previously in system A. System A had four B53 windows immersed in de-ionized water with a mean conductivity of 6.21 $\mu\text{S}\cdot\text{cm}^{-1}$, and a pH, measured at 20°C, of 7.26 ± 0.14 . The system B had also four B53 windows, immersed in “24-48 hour aged” water with a mean conductivity of 12.80 $\mu\text{S}\cdot\text{cm}^{-1}$, and a pH, measured at 20°C, of 7.12 ± 0.02 . An non-immersed window was used as a reference standard for weighing purposes.

2.2.2. “Five Day” Trials

Three B53 glass windows and three X-glass windows (also called E47.2 by ETL) were immersed in de-ionized water for a period of five days at various temperatures in the range of 30°C to 85°C. The B53 samples were immersed at temperatures of 73.0 and 82.6°C and the X-WINDOW samples were immersed at temperatures of 33.2 and 73.0°C. The mean conductivity was 3-12 $\mu\text{S}\cdot\text{cm}^{-1}$.

The apparatus was similar to the one used for the 30-day test with the exception that windows were fixed in position and mounted vertically using polypropylene fastenings in order to maximize exposure of both faces to attack by water. Also, glass types were separated based on composition and the de-ionized water was not recycled between beakers.

2.3. Results and Analysis

2.3.1. Results for B53 Glass Windows – “Thirty Day” Immersion Trial

The weight loss in system B is greater than the weight loss in system A throughout the experiment, and this is likely to be due to the greater conductivity of the water in system B, however the increased dissolution rate is relatively small (10-30%). The dissolution rate decreases by a factor of 2.5 to 3 during the experiment. A possible explanation is that the weight loss mechanism evolves from rapid ion exchange with the water-electrolyte into slow dissolution of the lattice.

Taking the average weight loss per day per unit surface area of B53 glass as $1.36 \cdot 10^{-05} \text{ g.day}^{-1}.\text{cm}^{-2}$ for system A (the surface area of the tested windows is 14.6cm^2), and the surface area of a typical window sealed onto a PMT tube as 7cm^2 , then the weight loss for the active surface area of the window is 0.1 mg/day at 83.5°C or 0.005% of the typical mass of a window (2 grams). This is equivalent to an average daily loss of thickness of 57 nm.day^{-1} , or 0.005% of the original window thickness (see Table 2).

Table 2. Weight Loss of B53 glass windows (mg).

	Day 0	Day 10	Day 21	Day 31	Uncertainty
Ave. weight of window (A)	1 946.44	1 943.27	1 941.48	1 940.29	0.05
Ave. weight of window (B)	1 903.92	1 899.61	1 897.66	1 896.27	0.05
Ave. weight loss / window /day (A)		0.317	0.163	0. 119	0.01
Ave. weight loss / window /day (B)		0.431	0.178	0. 139	0.01

2.3.2. Results for B53 and X-Glass Windows – “Five Day” Immersion Trials

As the dissolution of glass is generally slow at ambient temperature, it is conventional to measure the glass dissolution rate V at more than one elevated temperature T . The results can then be modeled using the Arrhenius equation in order to derive the activation energy Q for dissolution of the glass: $V = V_0 \exp(-Q/RT)$, where V_0 is the baseline dissolution rate and R the universal constant. So a plot of $\ln V$ against $1/T$ produces a straight line graph of slope $-Q/R$. The acceleration factor at increased temperature is deduced and then used to predict the performance of the glass at ambient temperature.

The measurements performed at different temperatures are shown in Table 3.

Table 3. Average weight loss per window and per day after five days immersion (mg).

	33.2°C	73.0°C	82.6°C	Uncertainty
X-glass window	0. 32	2.87	N/A	0.02
B53 glass window	N/A	0.33	0.64	0.02

Table 4 presents a comparison of the dissolution rate results for B53 windows during the five-day and thirty-day immersion trials at $\sim 83^\circ\text{C}$. The dissolution rate for the five day immersion trial is higher than the rates measured in the thirty day trial. This is as expected as the five-day trial will favor the initial ion-exchange weight-loss mechanism that will be faster than lattice dissolution. The analysis of the dissolution rates using data from the thirty day trial uses the average dissolution rate for simplicity, though it is noted that more sophisticated models of the dissolution rate could be constructed from these results.

Table 4. Average dissolution rates for B53 glass windows for the “five day” trial at 82.6°C and “31 day” trial at 83.5°C (10^{-5} g.day⁻¹.cm⁻²).

5 day trial		31 day trial				
5 days	uncertainty		Days 0-10	Days 10-21	Days 21-31	uncertainty
82.6°C			83.5°C	83.5°C	83.5°C	
4.40	0.12	(A)	2.17	1.11	0.82	0.06
		(B)	2.95	1.22	0.95	0.06

Results for the activation energy and acceleration factors for the B53 and X-glass windows are calculated from the five day immersion study results and summarized in Table 5. The reference temperature used for the calculation of the acceleration factor **AF** is $T_{ref} = 20^{\circ}\text{C}$.² We can calculate an accelerator coefficient **c** allowing the calculation of the acceleration factor at different temperatures with regard to a given reference temperature by the following formula:

$$AF(T) = c^{((T-T_{ref})/10)} \quad c = AF(T)^{(10/(T-T_{ref}))}$$

Table 5. Activation energy **Q**, accelerating factor **AC**, and acceleration coefficient **c**.

Temperature T [°C]	Activation Energy Q [kJ/mol.]	Acceleration Factor AF	Acceleration Coefficient c
B53 glass			
82.6	71.2	170	2.27
X-glass			
73.0	485	21	1.78
83.5		34	

2.3.3. Pressure Test

ETL selected ten PMTs and removed 2% of the front window thickness using air jet alumina powder. These ten PMTs were then immersed in water for one hour at 2.8 atm and survived the test. According to the manufacturer’s experience, this test is equivalent to more than 20 years of operation at normal pressure. This principle has been used by the SNO experiment to test the strength of their large PMTs.

2.3.4. Tests determining that the “frosty” PMT glass is a wrong type of glass.

TLC immersed six PMTs in 84°C water with partial circulation (three PMTs in the first tank, and the other three in the second tank, and daily fresh water was added in the first tank, and old water went into the second tank). Voltage was off during this test. In addition, four B53 glass coupons were placed in the first tank, and four B53 coupons into the second tank. The tests lasted 30 days. At the end of this period, five PMTs were partially “milky” and one PMT was “frosty.” The window coupons were slightly “milky” on both surfaces. The window coupons showed no transmission loss (measured in Saclay), and QE of one “milky” PMT (S/N262438) showed no significant change. However, QE of the “frosty” PMT (S/N 268885) was significantly different from the measurement before water exposure. In addition, the weight loss in the windows was $\sim 6\text{g/m}^2$, and the weight loss of the “frosty” PMT was $\sim 90\text{g/m}^2$. Table 6 shows the chemical composition of various glasses as measured by back-scattered X-rays.

The column labels in Table 6 have the following meaning:

- (a) B53 is data sheet composition of B53-type glass,
- (b) A is B53 glass from the batch supplied to DIRC group (not immersed in water),
- (c) B is B53 glass from the batch supplied to DIRC group (after 30 days in water at 84°C),
- (d) X is “low background” glass used in other PMT types at ETL,
- (e) C is from “frosty” window cut off from PMT S/N268885 after 30 days in water at 84°C (inside surface),
- (f) D is from “frosty” window cut off from PMT S/N268885 after 30 days in water at 84°C (“frosty” outside surface).

² The SOB water-return temperature is typically 26-28°C.

Table 6. Chemical composition of different PMT glasses used in ETL tests:

Analysis	B53	A	B	X	C	D
SiO ₂	65.5%	62.7%	66.1%	69.6%	74.3%	92.4%
NaO ₂	7.7	7.5	1.0	8.7	7.9	0.9
Al ₂ O ₃	6.2	6.8	7.3	4.2	4.1	5.1
ZnO	2.0	2.9	2.7	0.0	0.0	0.0
BaO	3.0	3.1	2.4	0.0	0.0	0.2
CaO	0.5	0.7	0.8	0.0	0.0	0.7
B ₂ O ₃	15.0	15.9	19.1	17.2	13.3	0.0

The conclusion from tests (e) and (f) is that the “frosty” PMT window (S/N 268885) is not B53 glass (it has no Zn) and is most probably X-glass. According to ETL, the B53 glass turns “milky” with the loss of sodium, while the “frosty” window has lost sodium and boron. **Therefore, it is argued that some DIRC PMTs turned “frosty” because a small number of X-glass windows mistakenly were mixed with the B53 glass windows in the DIRC PMT production.** Thus far, the company has not produced an independent estimate indicating how many PMTs with the “wrong” type of glass are in the DIRC. Figure 2 shows (see also section 2.3.5) the extent of the corrosion in “frosty” and “milky” PMT windows (cross-sectional view). One can clearly see that the “frosty” corrosion is much larger. The “frosty” window shows a uniform depth of attack up to 15% of the window thickness after 30 days in 84°C water. The depth of the attack on the “milky” window is entirely concentrated on the surface and it is too thin to be resolved optically even after 30 days in 84°C water. Figure 3(a) shows that there was no effect on the QE measurement of “milky” PMT; however, some effect on “frosty” PMTs as seen on Fig. 3(b). Figure 4 shows a correlation between the “frosty” PMTs removed from the SOB in the October 1999 shutdown and ETL’s serial numbers. It would appear that the largest group came as a cluster or two, which indicates a bad batch and a continuous problem.

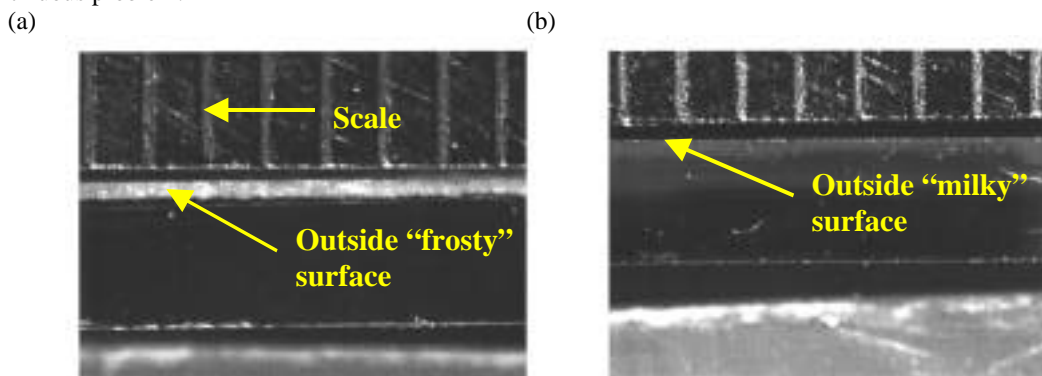


Figure 2. (a) Image of a sectioned X-glass window cut from a PMT after immersion in de-ionized 83.5°C water for 31 days. The thickness of the frosted region is 0.018 cm. (The rule spacing is 0.5 mm). The crazed edge is observed at the top. (b) Image of a sectioned B53 window cut from a PMT after immersion in de-ionized 83.5°C water for 31 days. There is no evidence of penetrative etching of the glass. The “milky” side is on top.

2.3.5. Discussion of ETL Results

The acceleration factor and the weight loss data from the five day trials can be used to calculate that 0.7% of the B53 window thickness will be lost after immersion for ten years at 20°C. If the weight loss data from the 31 day trials is used with the same acceleration factor, then approximately 0.1% of the window thickness will be lost. The difference between these two predictions is most probably due to the changing mechanism of weight loss from the glass as a function of time from ion exchange to congruent lattice dissolution. As ETL considers that there is a significant risk of implosion if greater than 50% of the window thickness is lost; there is

negligible risk of failure for PMTs with B53 windows. This is confirmed by the image of a sectioned B53 window, which shows no etching after 31 days at 83.5°C, equivalent to 14 years at 20°C [see Figure 2(b)].

X-ray fluorescence analysis of the surface of X-glass windows has shown that ion exchange or penetrative etching, as shown on Figure 2(a), dominates the weight loss mechanism. The X-ray analysis has been combined with the five-day weight loss measurements and the relevant acceleration factor to derive the 10 year etch depth as 48% of the original window thickness. Given that the calculated acceleration factors may vary depending on the local environment, the calculations suggest there is a sizeable risk of failure of the X-glass windows after 10 years.

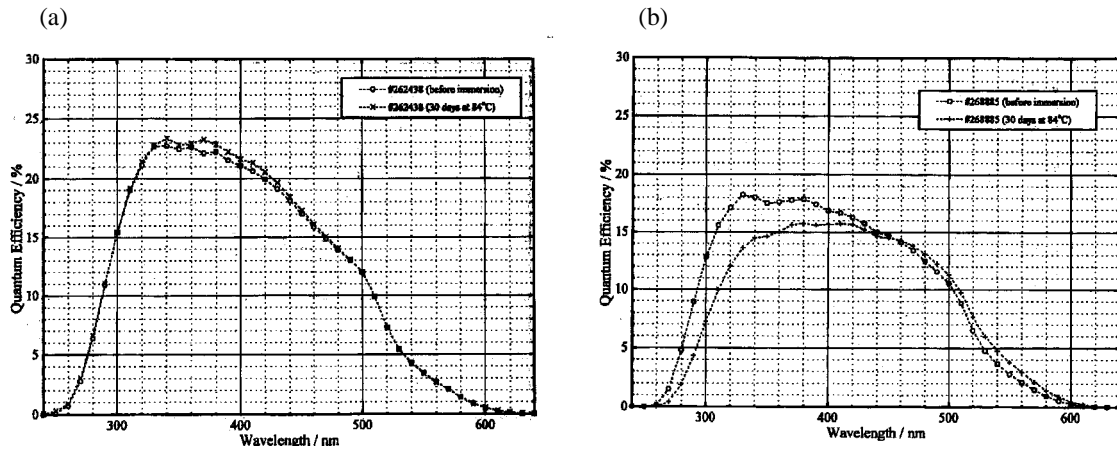


Figure 3. (a) No effect on measurement of QE of “milky” PMT exposed to water at 84°C for 30 days. (b) Some effect on measurement of QE of “frosty” PMT exposed to water at 84°C for 30 days.

Frequency of 'frosty' PMTs in bins of 500 delivered

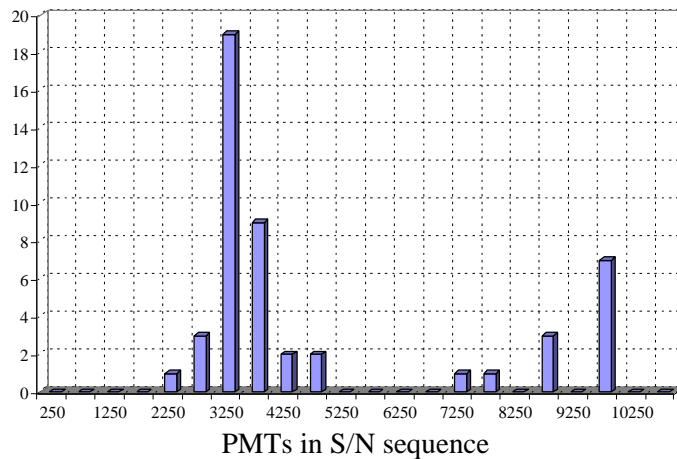


Figure 4. ETL company’s estimate how the “frosty” PMTs taken out of SOB correlate with serial number production. It appears that most of them came as one bad batch.

2.3.6. Conclusion of ETL Tests

The acceleration factors calculated from the five-day immersion trials predict that PMTs with B53 glass windows will lose less than 1% of the window thickness after 10 years immersion at 20°C. Therefore, there is no significant risk of envelope failure for PMTs with B53 windows.

The analysis of X-glass windows shows that up to 50% of the window thickness may be compromised after immersion for 10 years at 20°C. Therefore, there is a sizeable risk of implosion after 10 years for PMTs with X-glass windows. It is likely that the etching rate may vary in differing environments, so it is suggested that a PMT with an X-glass window could be removed and sectioned to determine the local etch rate.

The analysis of DIRC “frosty” PMTs shows that the front window glass has the same composition as the X-glass, which were mixed with the B53 windows in DIRC PMT production by mistake. The X-glass has no Zn, which causes excessive depletion of Na and B elements, and subsequent corrosion. The “milky” PMTs are made of the correct B53 glass, which has a tolerable rate of corrosion over 10 years in BaBar. This means that out of 10 800 PMTs in SOB, only 50 are made of wrong glass.

According to ETL’s test results, all “wrong glass” PMTs would turn “frosty” by the time of the October 1999 shutdown, i.e., we would have counted them all. This is an extremely important statement because we do not have an independent method to estimate how many of X-glass windows we have in the system.

4. Tests Performed at Saclay

4.1. Overview

This section describes tests performed at Saclay [4]. Glass corrosion was not the main worry of the DIRC group initially, assuming that the manufacturer understood such problems well at this point of time, and we can simply specify when ordering PMTs [6]. Saclay performed only tests related to water pollution triggered by the PMT’s material, and the emphasis was made on the helium tests and the sensitivity to the magnetic field [7]. Initial PMT glass corrosion tests were performed in parallel to the light-catcher coating corrosion and the socket gluing tests in Orsay. No obvious visual effects on the PMT front glass were observed at that time. After the October 1999 discovery of PMT front-glass corrosion, one PMT from the Orsay sample was also analyzed at SLAC. It was found that there was indeed sodium depletion in the front-glass window; however, the glass was obviously the B53 glass, and did not suffer from the gross corrosion. Therefore, in retrospect, the problem, judged by visual observation only, would not have been discovered during the Orsay tests.

The main emphasis in the tests performed at Saclay was in the area of photo-detection, and to check also for weight and transmission losses.

4.2. Experimental Setup: Water Station

As the need to understand the long-term PMT glass behavior over 10-years of operation, the corrosion studies are performed in hot water in order to accelerate the effect, similarly to the above mentioned ETL tests. This method is typically used in the industry to study chemical and mechanical characteristics. For temperature increase by every 10 °C, an acceleration factor of 2-2.5 is obtained. This factor is entirely empirical, depending of what we are studying. In Saclay tests, we have used a factor of two as a conservative acceleration coefficient (see Section 4.3.2). As we discussed in Section 2.3.1, ETL Co. empirically measured the acceleration factors of 2.3 and 1.8 for the B53 and X-glass respectively, based on the weight loss rates at different temperatures.

A small ultra-pure water station, with a recirculation capability, is used in the Saclay tests. The water is filtered, de-ionized and goes through an UV lamp to kill the bacteria. The water resistance at the inlet of the test container with no circulation is ~4 M Ω , and ~18 M Ω after the purification. For comparison, the DIRC SOB water resistance is between 8 (return from SOB) and 18 M Ω (supply to SOB). We also measure the resistance and pH factor of water samples taken from the PMTs stainless steel vessel, containing seven PMTs, in similar geometry as in the DIRC.

The temperature in the purification station could not exceed 40°C. In order to keep a high enough temperature of the water in the vessel, we have not recirculated continuously. Instead, only 3 hours three times a day initially, and later only once a day after having tested that the water quality stays good enough (checking that the resistance is greater than 1 M Ω , and no bacteria peak absorption is observed in the water transmission).

The vessel has been put in a thermostatic box and we measured periodically the temperature at different levels (see Fig. 5). The supply water resistance was 19 M Ω , and 1M Ω to 10 M Ω in the vessel. The pH factor was close to seven after water purification, and about 6-7 in the vessel.

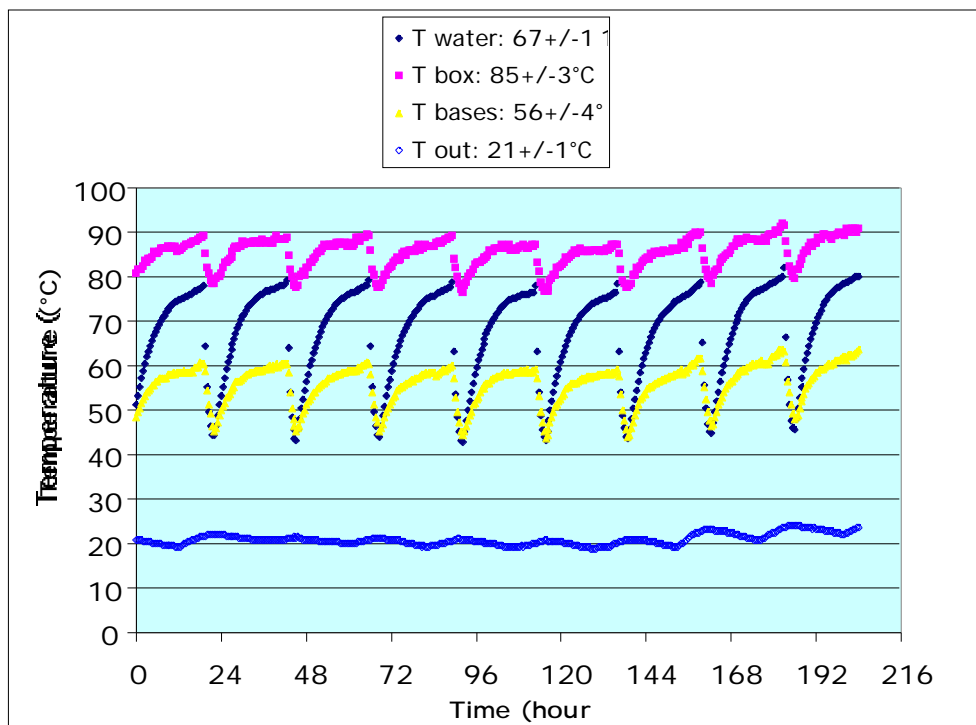


Figure 5. Temperature evolutions between two measurements on the PMTs, the average value of the water temperature has been used to determine the acceleration factor.

4.3. Experimental Setup: PMTs measurement

The seven PMTs were immersed in hot water and illuminated in the same manner as the DIRC PMTs during the calibration procedure [8,9,10]. We have used a blue LED, pulsed at 1kHz. To facilitate the measurement, we did not work at the single photoelectron level, but instead work with more than 10 photoelectrons in a Gaussian mode using directly the average value of the peak. To check the possible fluctuation of the LED, the light has been split and we have used a monitoring PMT (2020) at room temperature. The high voltage of the different PMTs (1140 to 1380 V) has been adjusted to have approximately the same LED amplitude. The LEDs were switched only during the measurement, but the PMTs have always stayed on.

The PMT gain correction due to temperature variation was calibrated out using a single-photoelectron peak measurement shown in Table 7 and Fig. 6, because of a possible PMT gain change towards the end of its life.

Table 7. PMT gain correction as a function of temperature.

PMT #	Slope (%/°C)
1	-0.55
2	-0.50
3	-0.33
4	-0.59
5	-0.37
6	-0.31
7	-0.34

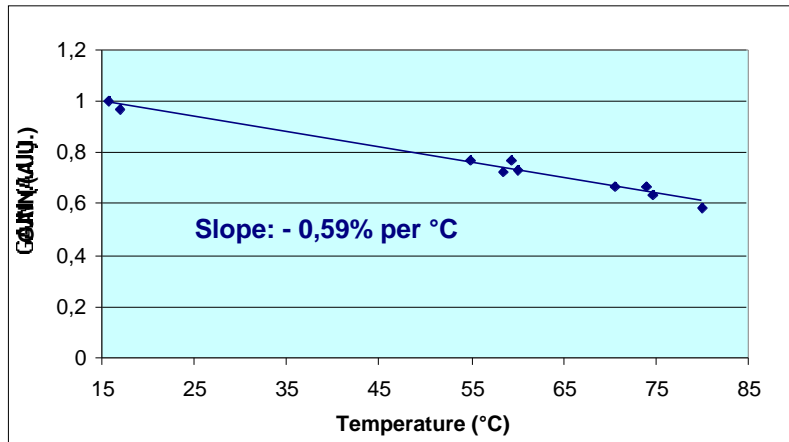


Figure 6. Normalized PMT gain versus the temperature of the water in which it has been immersed.

4.4. Results of the PMTs Corrosion

We have used nine PMTs, listed in Table 8. Two PMTs, #3 (“frosty”) and 7 (“milky”), were given to St. Gobain Company to analyze the composition of the glass to confirm the results of ETL.

Table 8. PMTs used in Saclay glass corrosion tests.

PMT #	PMT serial number	Origin
1	264829	Clear PMT removed in IR6
2	259755	Clear PMT removed in IR6
3	268882	Frosty PMT removed in IR2
4	255830	Milky PMT removed in IR2
5	268886	Frosty PMT removed in IR2
6	258106	Clear PMT from Orsay
7	258203	Clear PMT from Orsay
3'	268887	Frosty PMT removed in IR2
7'	050372	ETL free PMT sample grounded at Orsay

Table 9. Saclay PMT glass corrosion test results.

Run	Start of test	End	Time (days)	Mean temp. (°C)	Accel. Time (months)	Observations
1	11/09/99	12/20/99	40	66.8	17	End of test of PMTs # 3 and 7
2	01/16/00	02/16/00	30	66.6	12	Start of test of PMTs # 3', 7' and four B53 windows
3	02/17/00	06/27/00	131	63.5	62	Death of PMT # 7' (grounded) Water changed on 03/23/00
4	06/28/00	07/28/00	29	66.2	11	Death of PMT # 5 (frosty)

The tests started in November, 1999 and ended in August, 2000. The “grounded” PMT #7' was dead after 110 days (52 months equivalent, SOB at 28°C). At the end and before its death, PMT #5, labeled as “frosty” in the SOB, started displaying the “Christmas tree” effect,³ which lasted about ten days. This caused some loss in

³ “Christmas tree” is a condition when a PMT starts shining light uncontrollably. ETL explains that such condition may occur when either a PMT vacuum is slightly compromised or internal breakdown occurs [11].

PMT response due to loss of gain⁴ and efficiency. However, we cannot be certain if the efficiency loss is due to the quantum efficiency loss, or due to the transmission loss given that the photon flux was not calibrated absolutely. Table 9 shows the corrosion test results before the “Christmas tree” effect started.

We have taken pictures of PMTs at different stages of the corrosion test - see Figures 7-10. One can see that four clear PMTs become rapidly milky, followed by scratches appearing on the window surfaces. The “frosty” PMTs become more and more frosted, including the edges of the window. One can also see that the characteristic color of the photocathodes disappear on the dead PMTs, as if the surface was wet.



Figure 7. Seven PMTs, as they appeared before the beginning of the corrosion test. One can see four “clear” PMTs on the bottom, two “frosty” on each side, and one “milky” at the top right-hand side.



Figure 8. The same PMTs as in Fig. 7, after the first immersion in hot water for 40 days (equivalent to 17 months at 28°C). Notice that four “clear” PMTs became “milky”.

⁴ PMT 9125 PMT aging, which is a slight decrease of output in time, is due to: (a) When the PMT is on, the dominant mechanism is a change in gain approximately linearly with charge drawn. Typically the gain decreases to 50% after an anode draws a charge in the range of 200-400 Coulombs. (b) When the PMT is off, the quantum efficiency also degrades with the same 200-400 Coulombs half-life. Given that the cathode current is many orders of magnitude smaller than the anode current, the loss of quantum efficiency is usually negligible in comparison to the gain [12].

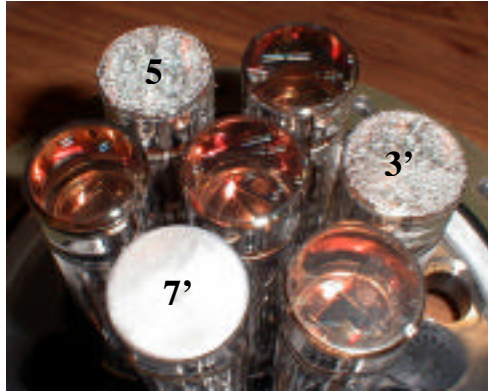


Figure 9. The same PMTs as in Fig. 7, after the second immersion in hot water for 30 days (equivalent to 12 months at 28°C). Scratches appeared on four “milky” PMTs, and edges of the “frosty” PMT # 5 also became “frosty.” It is the first immersion for PMT #3’ and 7’.

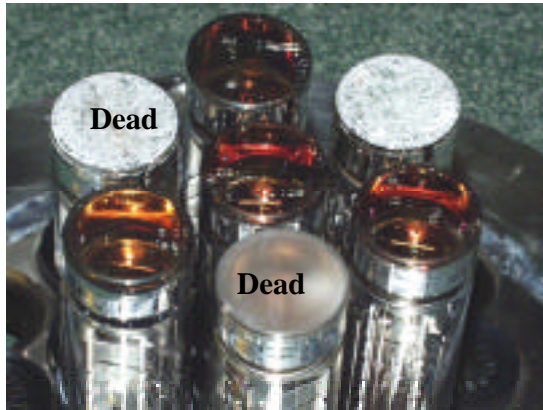


Figure 10. The same PMTs as in Fig. 7, after the third and fourth immersion in hot water for 174 days (equivalent to 82 months at 28°C); it is the second and third immersion for PMT #3’ and 7’. There are more scratches on four of the “milky” PMTs and the “frosty” PMT appears much more “frosty” when dry.

The results of the detection efficiency measurements with the LED flasher are summarized on Fig. 11. The data shows an overall drop in response, although one can see an initial increase in several PMTs. This increase is not entirely understood. One possibility is that some of the PMT front-glass was not entirely clean and the pollution washed away slowly (these PMTs were used at CERN in another test). A reason why we believe in this hypothesis is that the PMTs kept in clean conditions, such as the PMTs removed from the SOB, did show the initial rise in response. A less likely, although still a possible explanation of the initial increase in response is that the PMTs operated at high temperature during the test and some developed instability due to the evaporation of photocathode and/or coating of other surfaces. In any case, after certain point in time, all PMTs show a gradual drop in response to the LED photon flux (PMT #3 showing the smallest slope). The time used in Fig. 11 is the accelerated time calculated using the mean temperature and the acceleration factor of two per 10°C, taking 28°C as a reference temperature of the SOB. Using the mean temperature between two measurements introduces a systematic error of about 25% (we have done the exact calculation on 200 hours and found an accelerated time of 164 days instead of 131 days calculated with the mean temperature). Another point is that we have also used one acceleration factor for two different types of glasses.

Table 10 summarizes the results shown in Fig. 14, taking only the downward trend into account. The PMTs with B53 glass have an efficiency loss of 0.16-0.51% per month, which would translate to a loss of response of 19-61% in ten years. The loss in response is not only due to the window transmission loss but probably also due to photocathode aging. The gain change was corrected using a single-electron gain measurement.

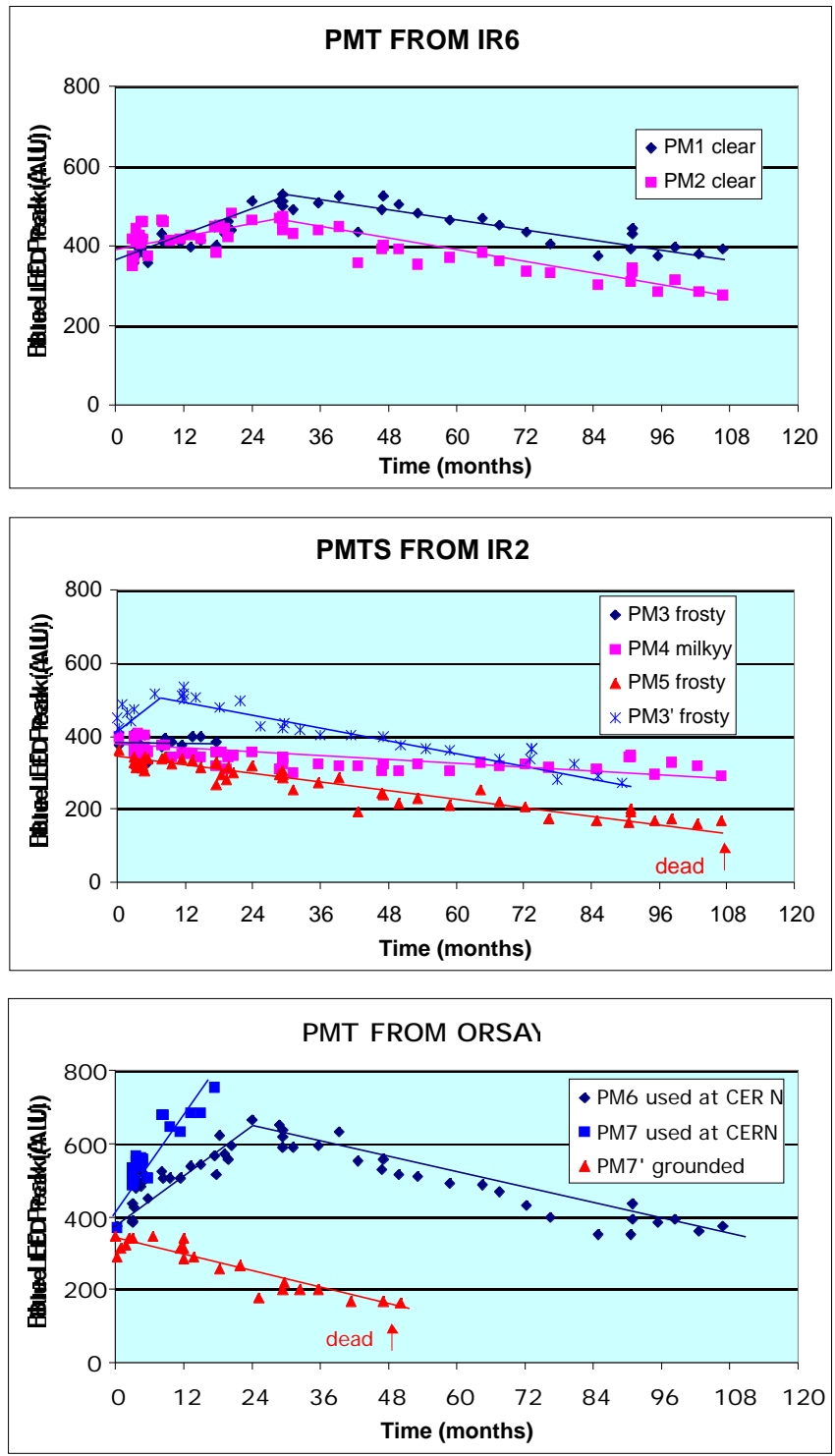


Figure 11. The PMT detection efficiency change as a function of time. Time was scaled to the SOB temperature of 28°C (taking into account the acceleration factor). The PMT response was measured using the blue LED producing ~10 photoelectrons on average.

Table 10. Slope describing the downward trend in PMT efficiency in Fig. 11.

PMT #	Condition	Slope (%/month)
1	Clear, then milky	-0.33
2	Clear, then milky	-0.39
3'	Frosty	-0.48
4	Milky	-0.16
5	Frosty	-0.53
6	Clear, then milky	-0.51
7'	Grounded	-0.96

Figure 12 shows that average number of Cherenkov photoelectrons per ring, as reconstructed from the Bhabha events, drops steadily as a function of the BaBar run number with a slope of 2-3%/year [13]. A similar result, shown in Fig. 13, was obtained from the di-muon events [14]. Both of these results confirm that we are probably dealing with a real loss of efficiency in the DIRC detector. Although these two results are still preliminary, it suggests a possible correlation with the Saclay results shown in Fig. 11.

The PMT gain drops after a certain accumulated anode charge is collected. For example, we can estimate the average anode charge assuming a BaBar run of 12 months duration, rate of 100kHz/PMT, the average single photoelectron pulse of ~25mV amplitude and 10ns duration, on a 50 Ohm load. We obtain the total anode charge of ~8 Coulombs per PMT per year. If we use the information disclosed [12] in Footnote 4, we may be actually consistent with the measured 2-3% efficiency drop shown on Figures 12 and 13, i.e., the observed efficiency drop is due to the PMT gain drop, i.e., due to a dynode aging process. If the efficiency loss is due to the PMT gain loss, and as long as it is only 2-3% loss per year, it can be easily corrected by a voltage adjustment. However, allowing large charge doses, for example the “Christmass tree“ effect, for a long period of time could be dangerous. On the other hand, the cathode accumulated charge is a tiny fraction of the anode charge (for the above axample is only $\sim 4.6 \times 10^{-7}$ Coulombs/year), which indicates that we probably are not dealing with cathode quantum efficiency drop at BaBar.

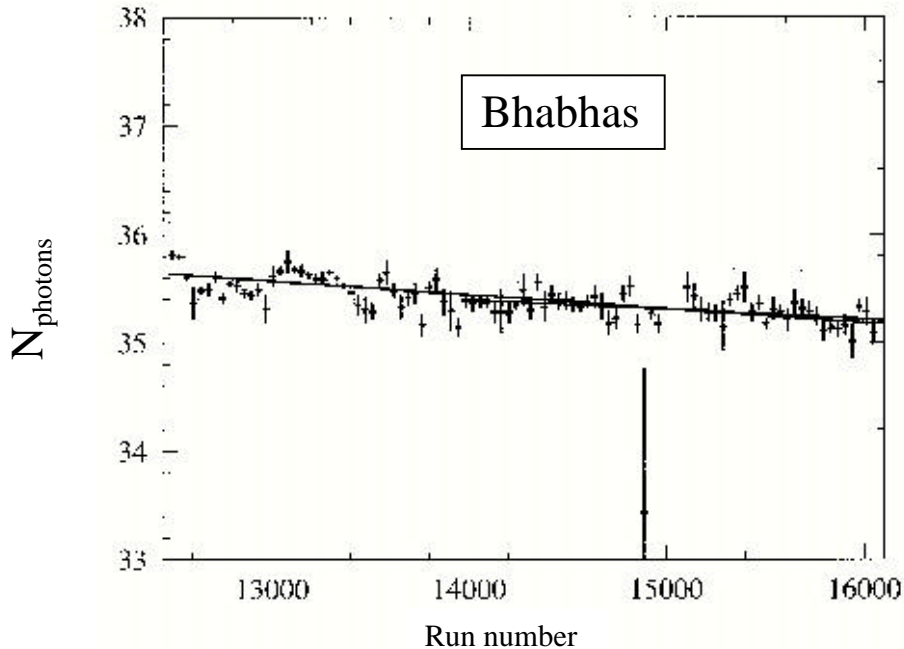


Figure 12. Average number of Cherenkov photons per ring from Bhabha analysis as a function of the BaBar run number [13]. The decline is consistent with 2-3%/year.

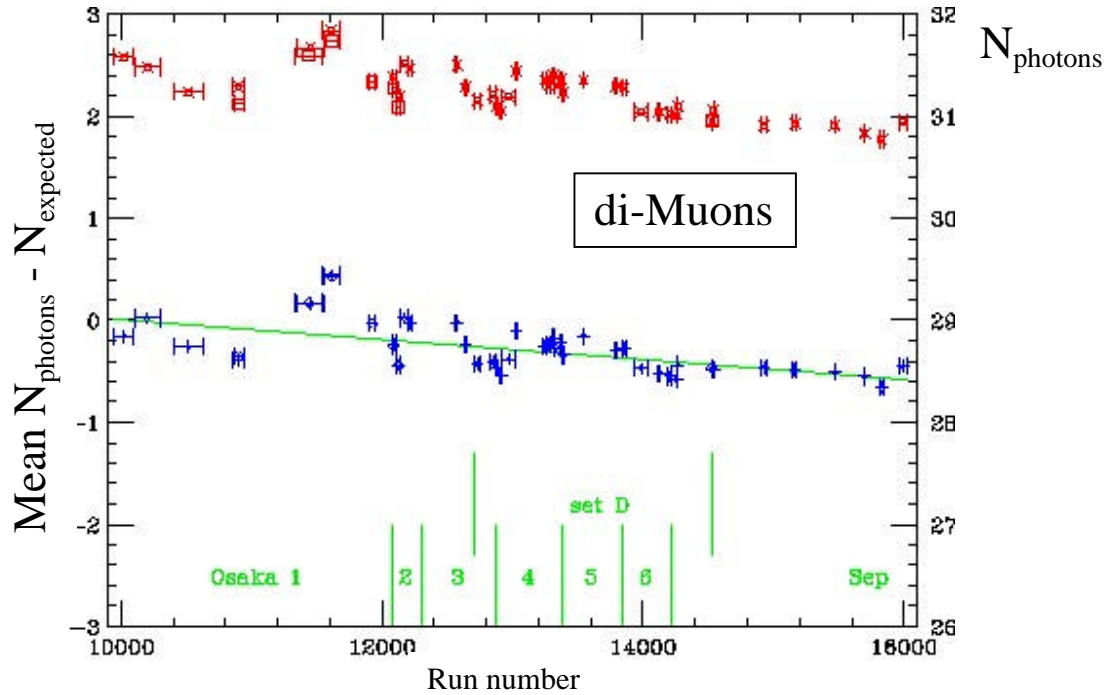


Figure 13. Average number of Cherenkov photons per ring from di-muon analysis (x points) as a function of the BaBar run number [14]. The figure also shows a relative difference from the expected number (+ points). Both curves indicate a decline at a level of 2-3%/year.

4.5. Weight and Transmission Loss

The weight loss measurement was done using front window coupons of B53 glass obtained from ETL Co. Four coupons were placed vertically in the PMT vessel, attached to three pieces of PVDF hose used for the water system, as shown in Figure 14.



Figure 14. Four B53 glass window coupons with supports.

We have performed two kinds of measurements: (a) the weight loss using a 0.1mg accuracy scales (Sartorius), and (b) the transmission loss between 200 and 850 nm (the spectrometer was made by Perkin

Elmer, Lambda 16). We have also taken pictures and seen milky spots, at the beginning only at the level of the hose contact, then more and more scratches (see Fig. 15).

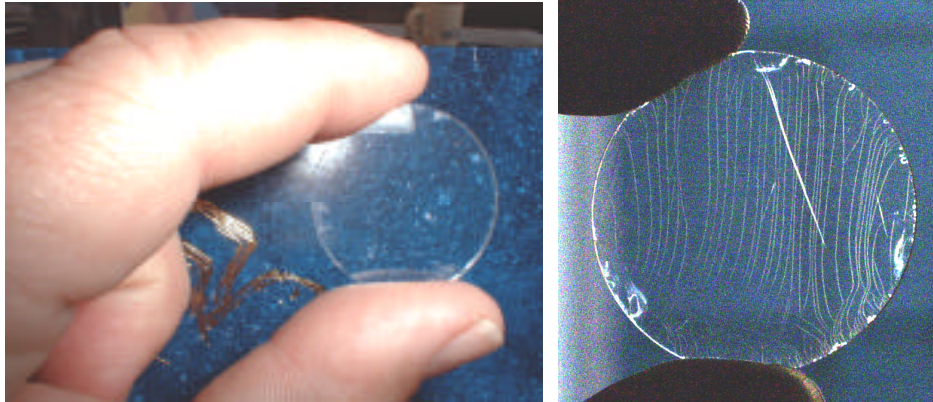


Figure 15. (a) B53 glass window coupon after the first immersion in water, and (b) after the third immersion.

4.5.1. Weight Loss Measurements

We have compared our results with those of ETL. They are not completely in agreement, as we have not done the test in the same experimental conditions. For example, the temperature is higher for ETL data, and the ETL water resistance is lower. Figure 16 and Table 11 summarizes the results of the measurements. The equivalent SOB time has been calculated with the acceleration coefficient of two, and the reference temperature of 28°C; this gives ETL an acceleration factor of 50. However, ETL's conclusion is still valid, i.e., the PMTs equipped with the B53 glass should not implode in 10 years of running.

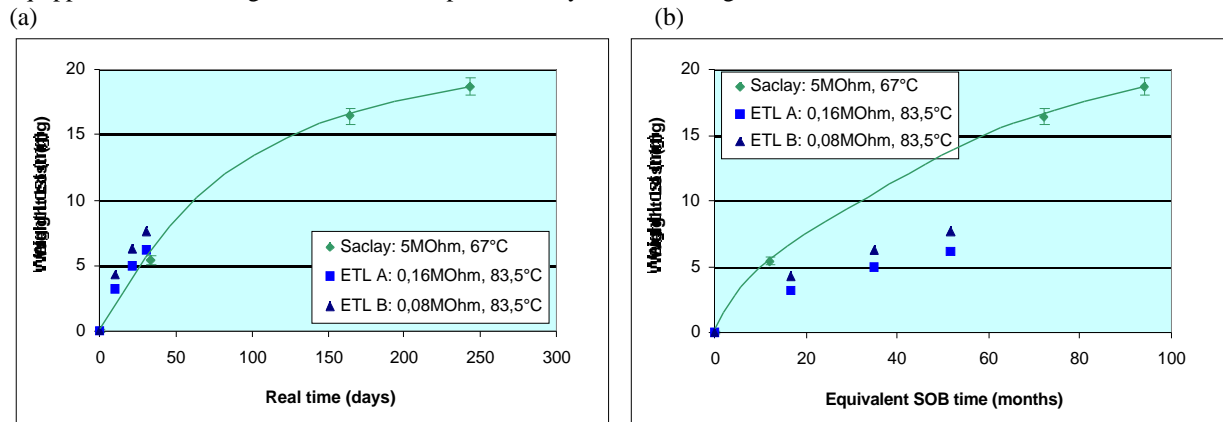


Figure 16. B53 glass coupon weight loss as a function of (a) the real time and (b) the SOB equivalent time

Table 11. B53 glass coupon weight loss measurements at Saclay and ETL.

SACLAY				ETL			
Real Time (days)	SOB Time (months)	Weight Lost (mg)	Error (mg)	Real Time (days)	SOB Time (months)	A (mg)	B (mg)
0	0	0.0	0.2	0	0	0.0	0.0
33	12	5.4	0.3	10	17	3.2	4.3
164	72	16.4	0.6	21	35	5.0	6.3
243	94	18.6	0.7	31	52	6.1	7.6

4.5.2. Transmission Measurements

Figure 17 shows the transmission loss as a function of wavelength for a reference glass coupon as well as one of four coupons immersed in hot water for different periods of time. Figure 18 shows the mean transmission loss (averaged over four coupons) at three wavelengths as a function of time. Note that corrosion takes place on both faces, so the transmission loss is greater here than in the SOB. Another important point is that the measurements were not done with water directly coupled to the corroded surface, which would definitely improve the transmission, even though the surface is visibly corroded. In that sense, this is a less important result, which is not directly applicable to the DIRC analysis. It only indicates that the glass surface is indeed corroded.

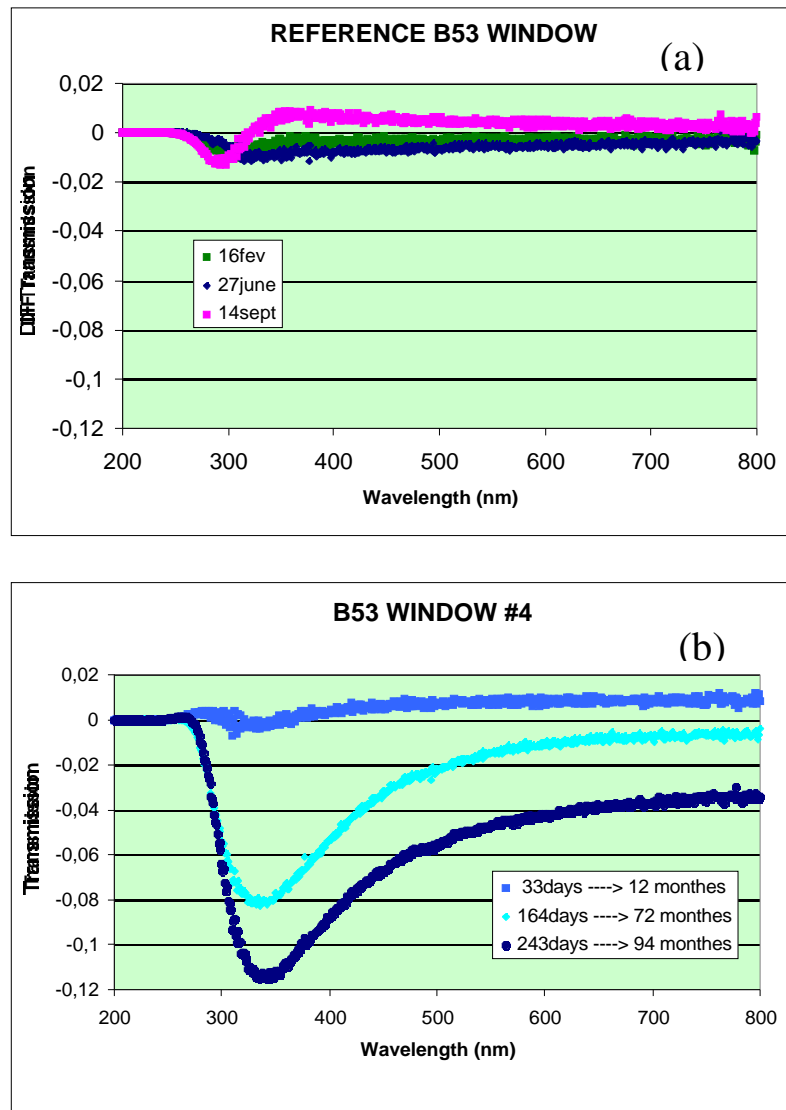


Figure 17. The transmission loss (relative to the initial transmission), for (a) the reference B53 window, and (b) for one coupon immersed in hot water for different periods.

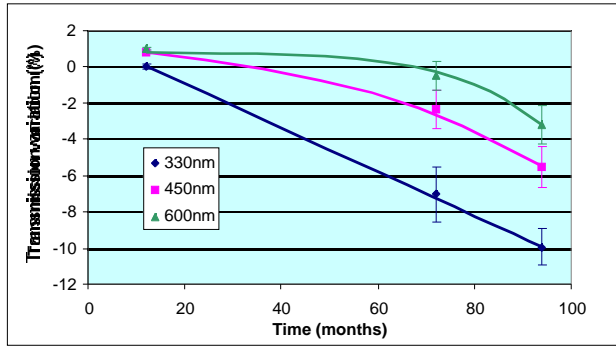


Figure 18. The transmission loss in % at different wavelengths.

5.6. Conclusions from Tests at Saclay

The effect of ultra pure water on the PMT glass window has been quantified by studying the corrosion rates in hot water and applying the relevant acceleration factor. We confirm the ETL results that the PMT front window, made of B53 glass, will lose less than 1% of its thickness in ten years of operation as a result of water attack. Therefore, there is no significant risk of implosion for PMTs with the B53C windows. Our measurements, based on scaling from the hot water tests, indicate that the risk of implosion is small in ten years even for the “frosty” PMTs. Saclay plans to make a cross-sectional view through the “frosty” PMTs.

We measure a decrease of a few percent in the transmission after ten years equivalent at SOB temperature. However, this measurement was done in air, where the optical coupling is much worse than in water.

We measure a non-negligible loss of detection efficiency, on which we can put an upper limit ranging from 20 to 60% per ten years of operation. The loss of the detection efficiency could be explained by a loss of either the window transmission or the PMT quantum efficiency (in this measurement, the PMT gain variation was calibrated out). The efficiency loss measured in Saclay would represent an addition to the possible PMT gain loss due to the total accumulated anode charge mentioned in Section 4.4. However, one should add that the Saclay test did not measure a possible loss of the quantum efficiency in warm water.

5. Tests Performed at SLAC

5.1. Overview

This section describes tests performed at SLAC. They include periodic visual observations of the status of PMT glass faces viewed through the window ports of SOB, taking pictures of PMTs removed from the SOB vessel, X-ray and ESCA surface analysis of PMT glass, detailed SOB water trace element analysis, a long-term test of front PMT glass coupons. We used the water analysis to check if the sodium and boron levels are consistent with the known corrosion of the PMT glass. We also include other measurements, which SLAC performs regularly, such as the water transmission at 266, 325, and 442nm, water pH factor, water resistivity, and SOB water temperature. The result of this work is described in the following sections.

5.2. Visual Observation of PMT Glass Through the Ports in SOB Vessel

We can only see gross effects when viewing a corroded glass through the SOB port, while the vessel is full of water. This is because of very good optical coupling of water to glass surface, even if it is corroded. We have performed periodic checks over the past ten months. There was no observable degradation detected.

5.3. Electron Microscope Pictures of PMTs Removed from the SOB Vessel

Figure 19(a) shows an electron microscope picture of a “frosty” PMT, designated as #4 in Fig. 1. The surface is full of small fractures, which seem to be peeling off the surface underneath. Some of the fracturing occurs when the PMT is subjected to vacuum forces in the electron microscope. For example, Figure 19(b)

shows an example of such fracturing on a “milky” PMT, designated as #3 in Fig. 1. It is believed that it occurred in the vacuum. The thickness of the fracture shown on Fig. 19(b) is 1-2 microns. Another example is shown on Fig. 20, which shows PMT #10, which was neither “milky” nor “frosty” and was removed from the SOB by mistake. It also developed crazing when subject to forces in vacuum. This indicates that any PMT, which was subjected to water for more than ~6 months, must not be stressed excessively in any way. This result led us to a major decision not to open the SOB unless absolutely necessary.

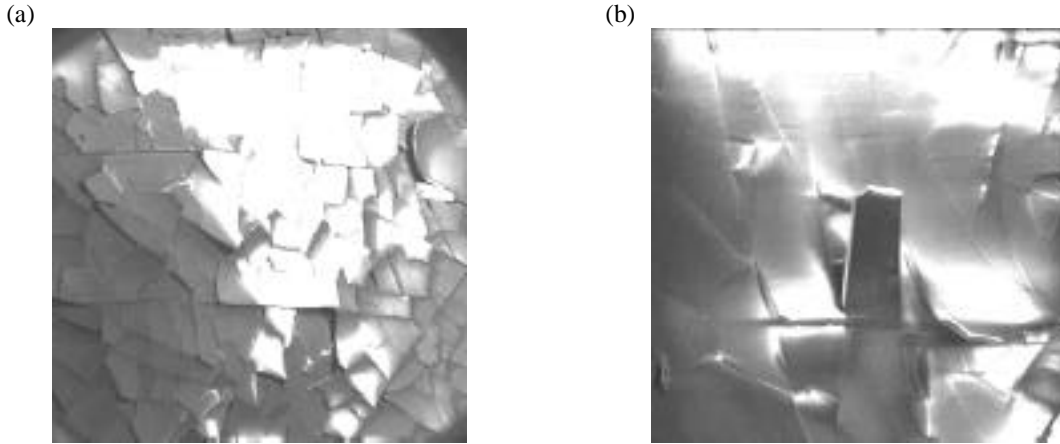


Figure 19. (a) “Frosty” PMT, designated as #4 in Fig. 1, developed crazing already in the SOB. (b) This picture indicates that a “milky” PMT, designated as #3 in Fig. 1, can develop crazing when placed in the electron microscope vacuum. The thickness of the fracture is 1-2 microns.

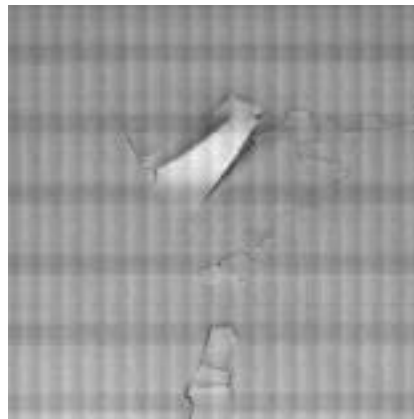


Figure 20. PMT #10, designated as “clear” and nearly perfect, was removed from SOB by mistake (it was neither “milky” nor “frosty”). It developed crazing when subjected to vacuum forces in the electron microscope. This led us to conclude that we should minimize any stresses, such as unnecessary water draining, SOB opening, etc.

5.4. Surface X-ray Analysis of PMT Glass

This technique uses an electron beam (~15 keV) and measures a spectrum of the recoiled X-rays. Figure 21 shows a typical X-ray spectrum taken at accelerating voltage of 15 kV. A simulation, shown in Fig. 22, shows the electron beam penetrating 1-2 microns in glass at 15kV, i.e., probing the few microns at the surface. At the same time, the electron beam lateral spread is about 1-2 micron when it stops. Therefore, a sampling volume at this voltage is a cube of the size of a few microns. This is an important result because several conclusions, based on the X-ray analysis and presented in Section 5.4.1, only apply to a tiny depth.

One can clearly identify major peaks of O, Na, Si, C, and Al in Fig. 21. These peaks will be used in Section 5.4.1 to analyze the sodium depletion in the front-glass. It is difficult to see Zn using our electron microscope, because the Zn and Na peaks are close to each other. At 15 kV, Zn has two X-ray lines, a dominant one is at 1.010 keV and a weaker one is located at 8.638 keV (less than 10% intensity). Na has only one line at 1.041 keV. This was verified by using calibration targets containing either ZnO or NaF₂. In all our PMT front glass analysis of “milky” or “frosty” tubes we did not have any hints of the 8.638 keV line, which would indicate a presence of Zn. One should add that there was no peak corresponding to Rhenium, which would indicate that the light catcher plating is coming off.

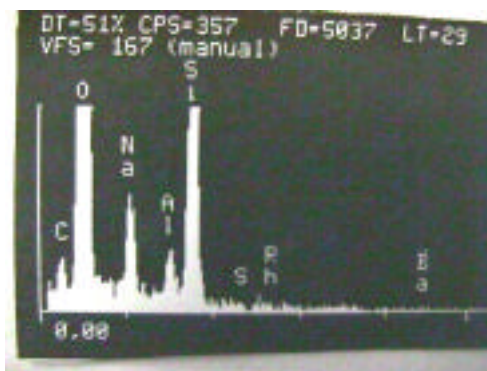


Figure 21. Elemental composition of a reference glass as measured in the electron microscope operating a 15 kV. electron beam strikes a PMT front glass surface and recoil X-ray spectrum is measured. One can clearly recognize major components of glass: O, Si, Na, Al and C.

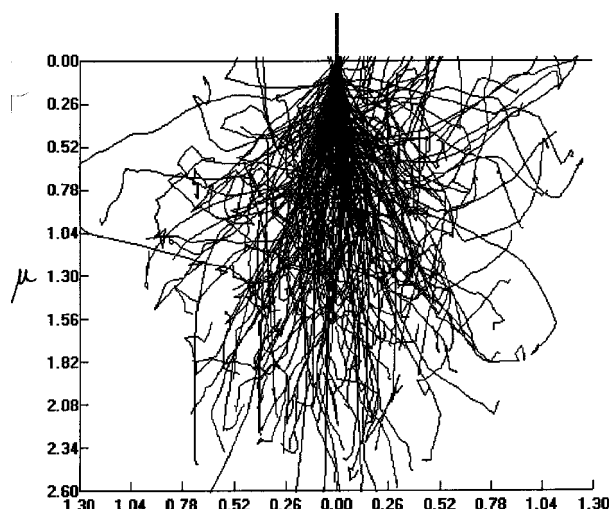


Figure 22. Monte Carlo simulation of motion of 15 KeV electron in SiO₂ using the commercial program “Flight Simulator” (courtesy of B. Kirby).

5.4.1. Sodium Depletion of PMT Front Glass Taken out of SOB Vessel

Figure 23 shows a sequence of points along the PMT envelope where the primary electron beam strikes. For each point we have taken, the X-ray spectrum is similar to that shown in Figure 21. As one follows the sequence of points, shown in Fig. 23, one slightly changes the solid angle for the X-ray detection. This was calibrated out by using a Na/Si ratio, assuming that the Si component is changing only slightly.

Figure 24 shows the result as a ratio of X-ray peak areas of Na and Si for a “milky” PMT #6 (S/N 050038) (taken out of SOB during the October 1999 shutdown), normalized by the same peak area ratio for a brand new PMT (this PMT was not immersed in the water at all). One can see that points 5-14, which are located on the

front PMT glass surface, clearly shows sodium depletion relatively to points 1, 2, 3, 4, and 15, which are located on the glass side of the PMT, as shown on Fig. 23. The side glass has a different composition than the front glass (see Section 6).

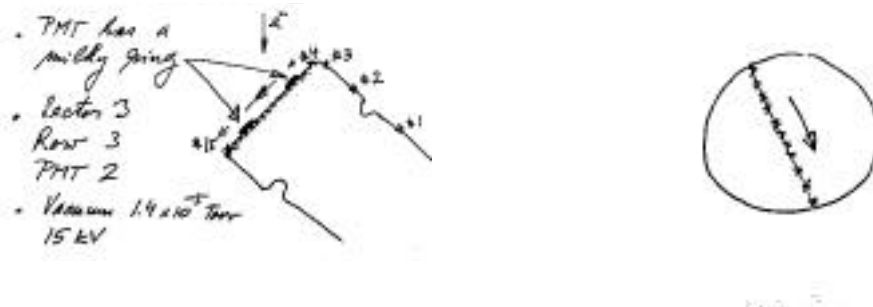


Figure 23. A sequence of points along the PMT glass, where the electron beam hit and the X-ray scan was taken to check for sodium depletion.

Another analysis performed under a flake of PMT #4, similar to that shown in Fig. 19(b), indicates no sodium depletion. However, on top of the flake sodium depletion is detected. Given the fact that a typical flake, as shown in Fig. 19(b), is only few microns thick, is indicative that the sodium depletion extends to depths of only a few microns. This result is consistent with the penetration depth of 15 keV electron beam in SiO_2 , as simulated in Fig. 22 by a computer program. The measurement of sodium depletion under the flake was possible since the PMT was placed into the electron microscope at an angle. The result is also consistent with the rate of removal based on the water purity tests described in Section 5.6.

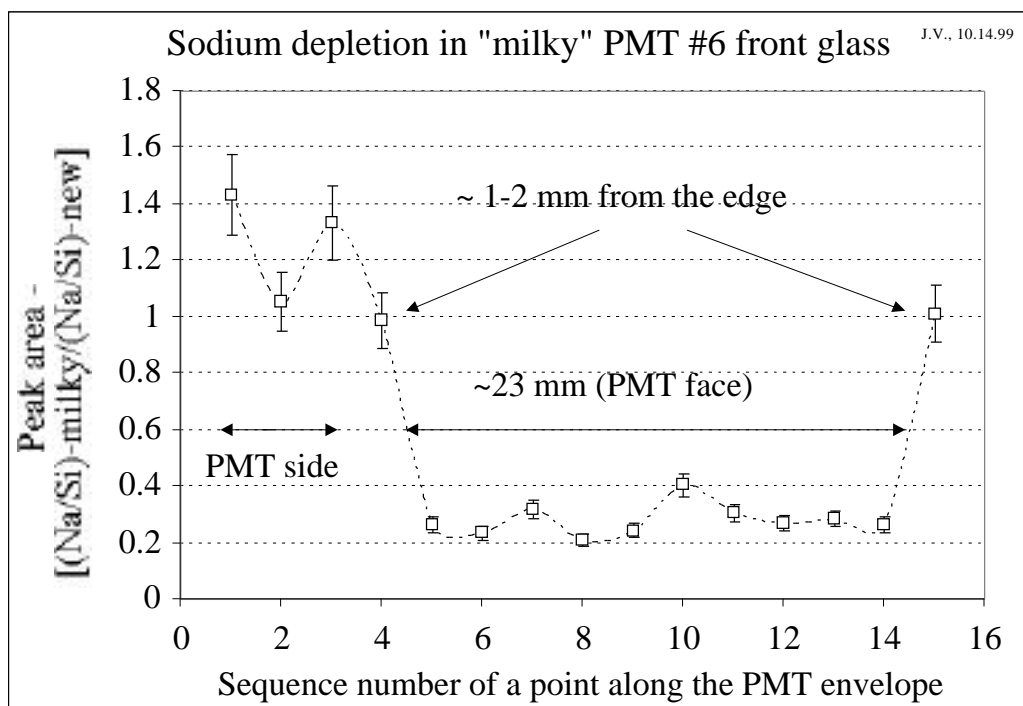


Figure 24. Sodium depletion in the front glass of PMT #6 (S/N 254776) judged as having a “milky” surface, and removed from the SOB during October 1999 shutdown. A sequence of numbers follows the glass envelope as described on Fig 23. The Si X-ray peak was used as the normalization of the X-ray detector response due to the changing solid angle during the surface sweep.

Figure 25 shows similar sodium depletion, although to a lesser extent. The front PMT glass surface (#1 or S/N 050038) used in early verification tests in Orsay, is designed to show that there is no water induced PMT glass corrosion. Indeed, one can confirm that there was no visual effect. However, more precise X-ray tests show that corrosion is present in terms of sodium depletion on the front of the PMT glass.

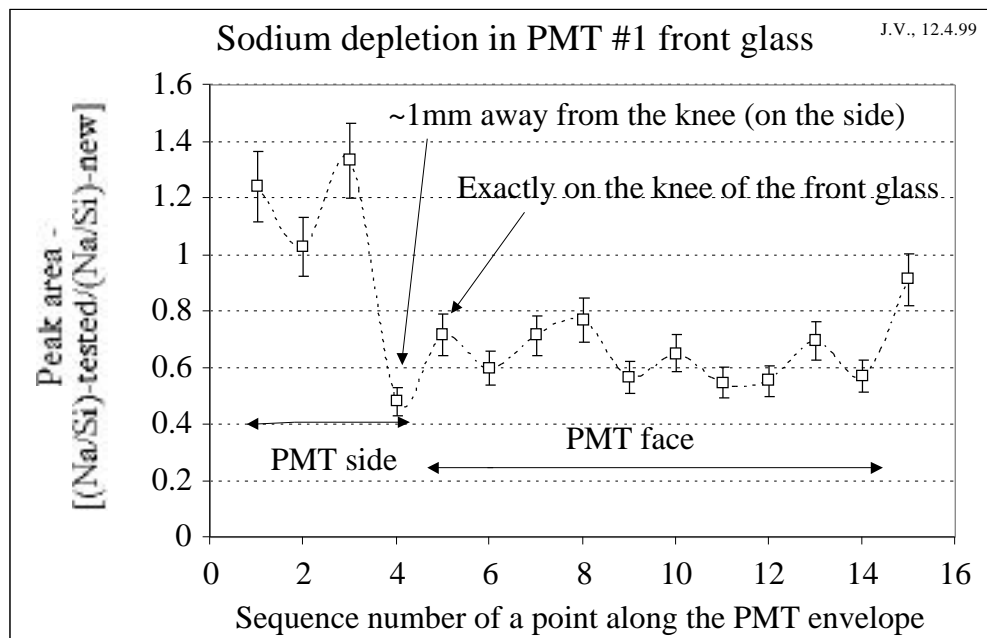


Figure 25. Sodium depletion in the front-glass of PMT #1 (S/N 050038) used in early tests at Orsay to verify the absence of the glass corrosion by water. A sequence of numbers followed the glass envelope is described on Fig. 23. The Si X-ray peak was used as a normalization of the X-ray detector response due to the changing solid angle during the surface sweep.

5.5. ESCA Analysis of the PMT Front Glass Taken out of the SOB Vessel

This technique uses a very soft X-ray beam (1.487 keV) and measures a spectrum of the recoiled electrons. The soft X-ray beam probes only $\sim 50\text{\AA}$ of the glass volume, which is a major difference from the electron beam-based X-ray analysis (see Section 5.4), which probes 2-3 microns of glass volume at 15kV. Another technical difference is that the ESCA spectrometer vacuum chamber is much smaller, and one needs to cut front PMT glass to do the front glass analysis.

The analysis was done on several tubes: (a) “milky” PMT #6 (S/N 254776), (b) “milky” PMT #8 (S/N 255140), and (c) “frosty” PMT #4 (S/N 268893). The last two were broken up to allow a cross-sectional analysis of the front glass. Figure 26 clearly shows that Zn is present in the front glass of the “milky” PMT #6, although we do not see any Na, because it is already depleted from the front surface. Figures 27 and 28 show that both elements, Zn and Na, are present in the “milky” PMT #8. This means that zinc is present not only on the outside surface (Fig. 27), but also in the volume (Fig. 28). This is evaluated as consistency proof that the “milky” appearance corresponds to B53-type glass, which confirms the ETL results. On the other hand, Fig. 29 shows that we clearly do not see Zn in the “frosty” PMT #4, although we do see Na. This agrees with ETL observation that only the “frosty” PMTs do not have Zn element in the front glass. The milky PMTs, as well as all clear PMTs, do have Zn in the form of ZnO. Our tests were done on PMTs taken out of the SOB vessel in IR-2 after being immersed in water for ~ 8 months at temperatures between 26-28°C.

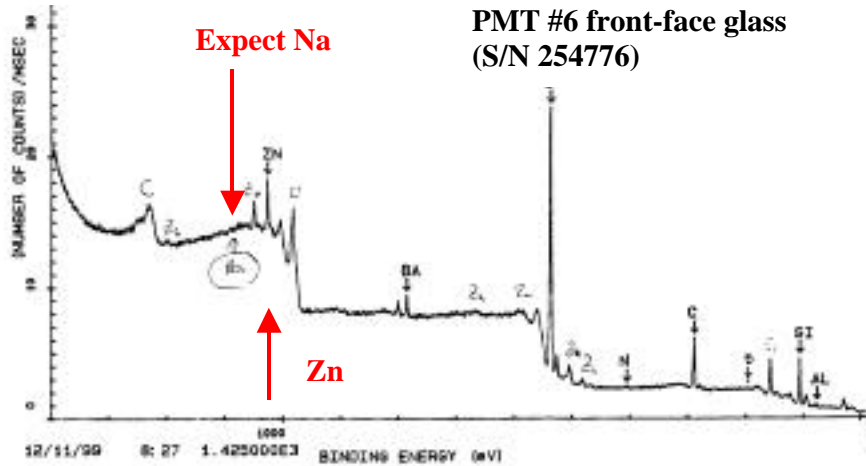


Figure 26. ESCA analysis of front face glass of PMT #6 (S/N 254776), which was judged as “milky,” and removed from the SOB vessel during the October 1999 shutdown. Zn is clearly detected, which is taken as a proof that the glass was indeed B53 glass, which is consistent with the “milky” appearance; however, there is no sign of Na.

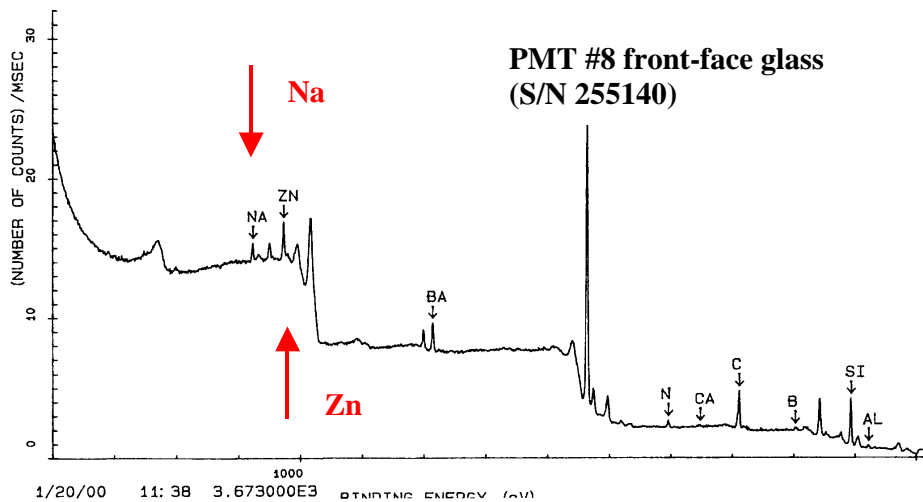


Figure 27. ESCA analysis of front-face glass of PMT #8 (S/N 255140), which was judged as “milky,” and removed from the SOB vessel during the October 1999 shutdown. Both elements, Zn and Na, are clearly detected.

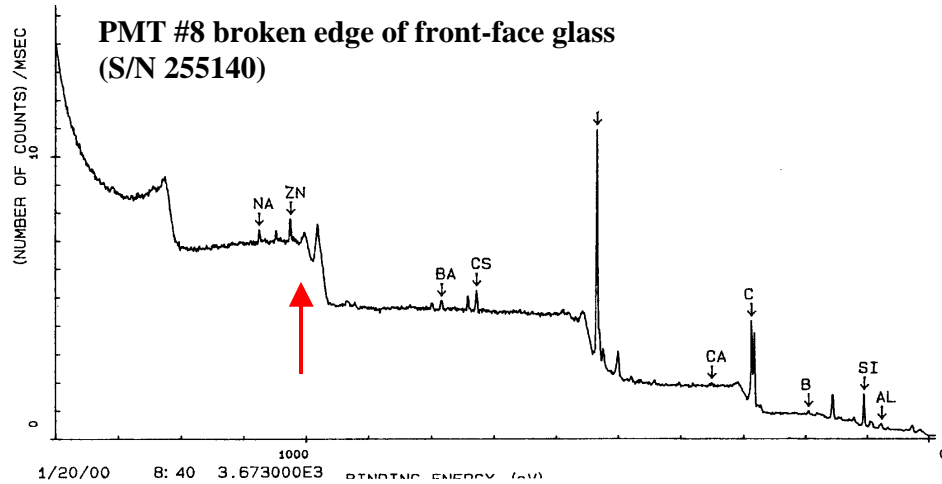


Figure 28. ESCA side analysis of the broken edge of the front face glass of PMT #8 (S/N 255140), which was judged as “milky,” and removed from SOB vessel during the October 1999 shutdown. Both elements, Zn and Na, are clearly detected in the volume of the front glass. This means that the glass is B53-type glass, which is the correct type of glass.

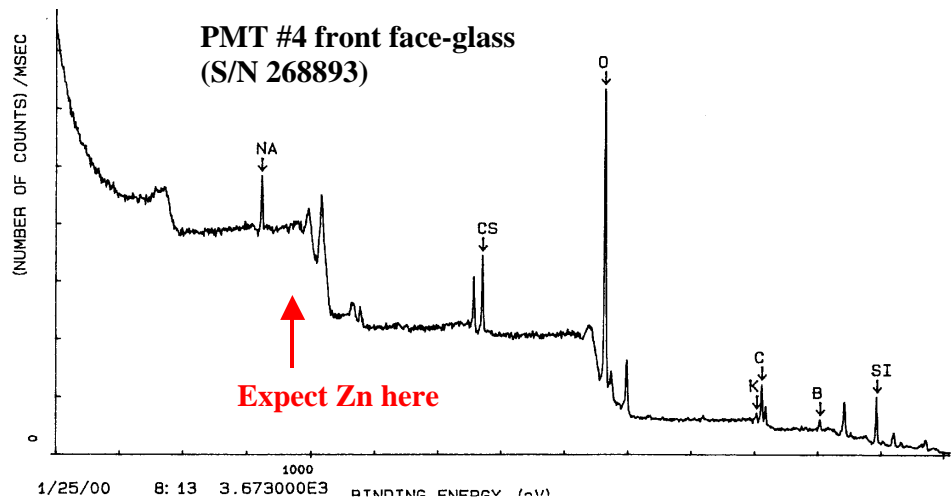


Figure 29. ESCA analysis of front face glass of PMT #4 (S/N 268893), which was judged as “frosty,” and removed from SOB vessel during the October 1999 shutdown. Clearly, we see no sign of Zn. This confirms the ETL observation that “frosty” PMTs do not have Zn element, because they have the wrong X-type front glass window.

5.6. Water Analysis and Its Relationship to Glass Corrosion

If elements of the PMT glass are leaching into water, we should be able to detect them in the precision water analysis. Today, a modern water analysis is capable of determining impurities at a level of 0.001-0.010 ppb. As we will see, with this level of precision it is possible to verify that sodium from the front PMT glass is indeed leaching into the water, i.e., verify conclusions from the X-ray analysis described in Section 5.2.1. By doing periodic water analysis, it is then possible to determine if the leaching is constant, improving, or deteriorating.

Table 12 shows the results of trace metal analysis, the detection limits and bacteria count in the supply and return SOB water in IR-2, performed ~8 months apart. Our experience with the detection limits indicate that the quoted number, especially frequently found elements such as sodium, could exceed its nominal quoted value by a factor of 2-3 on any given measurement trial. Variations can be caused by a sampling technique, presence of people, sample bottle contamination, etc. The water sampling and the analysis were done by the Balazs Co.⁵ We were especially interested in elements, which are present in the PMT glass, such as sodium, boron, and silicone. The difference between supply and return water samplings in November 1999 indicate 0.28 ± 0.14 ppb of Na, 0.3 ± 0.1 ppb of B, and 0.3 ± 1 ppb of Si, where the error margin is given as twice the detection limit shown in Table 1. In August 2000, these differences changed to 0.44 ± 0.14 ppb of Na, 0.4 ± 0.1 ppb of B, and 0.0 ± 1 ppb of Si. For all practical purposes, we can neglect Si as a significant result given its very large errors.

According to ETL, the B53 glass turns “milky” with the loss of sodium, while the “frosty” window has lost sodium and boron (see Section 2.3.4.). If we assume this, we may determine two different scaling. One for the sodium leaching from all PMTs in the DIRC, and another for the boron leaching from only “frosty” PMTs, which are made of X-glass. There are only 50 such PMTs in the DIRC system.

From Table 12, we conclude that the leaching rates of Na and B are, within errors, constant during the past eight months. We can also use the results from Table 12 to estimate the depth of the PMT front glass affected by Na and B leaching. Table 13 shows results of this calculation. The analysis of the Na leaching indicates that we are removing this element from the front PMT glass at a rate of 3-4 $\mu\text{m}/\text{PMT}/\text{year}$. This is consistent with the electron microscope surface analysis of the “milky” PMTs taken out of the SOB in October 1999. At this rate of removal, and assuming that it will continue to be constant in the future, the PMTs with B53 glass should last ~10 years from the point of view of the implosion danger. The analysis of the B leaching, assuming that boron comes out of “milky” PMTs only, indicates that we are removing this element from the front PMT glass at a rate of ~800 $\mu\text{m}/\text{PMT}/\text{year}$. This is much larger than what ETL has measured (see Fig. 2). At this rate of removal, the “frosty” PMTs would have already imploded. Clearly, the boron model’s assumption that only “frosty” PMTs leach it may not be entirely correct. It would be more consistent with our observations to assume that boron leaches similarly to sodium, i.e., from all PMTs with B53 glass (see Table 13 for details).

Table 14 shows SLAC’s measurements of the water pH factor, resistivity, transmission, and temperature during water samplings shown in Tables 12 and 13. Clearly, these variables are not sensitive to the level of impurities seen in the water analysis.

It is useful to compare the DIRC water quality with other experiments, for example, such as Super Kamiokande (SK) or K2K, which have been successfully running already for the past 2-4 years with a very large number of PMTs in ultra-pure water. Table 15 shows the impurity level in water of SK and K2K experiments, and this is to be compared with the DIRC water purity shown in Table 12. If one takes, for example, sodium in their water, it is comparable with our level, however, in their case, there is no evidence suggesting that they are leaching it from PMTs (supply is higher than return). Perhaps, one could argue that the K2K experiment could be leaching calcium and aluminum, both elements are present in their PMTs. However, there is no visual evidence of PMT window glass corrosion in these two experiments [15]. Table 16 shows their typical operating parameters, such as water flow, pH factor, resistivity, and water temperature. Judging from a similarity in water resistance between DIRC, SK, and K2K, it appears that the water quality is rather similar.

One thing to notice is that the SK and K2K experiments are running considerably cooler than we do, which certainly helps to keep the bacteria level low, and it also helps to reduce chemical reactivity of the water. A low bacteria level is important from the point of view of corroded surface. Bacteria “likes” to reside in various cavities, and we certainly would not want them to be “residing” in PMT window glass, which would reduce photon transmission. Therefore, it was pleasing to see low-bacteria count in the SOB water return during our last measurement – see Table 12.

⁵ Balazs Analytical Laboratory, 252 Humboldt Court, Sunnyvale, CA 94089-1315.

Table 12: Trace metal water analysis of DIRC water performed by the Balazs Analytical Laboratory.

Parameter	Test type	DL(det.lim)	Units	SUPPLY	RETURN	SUPPLY	RETURN
				11/30/99	11/30/99	8/21/00	8/21/00
Bacteria/100ml	Bacteria-ASTM		1 cfu	*,*,*	>500,>500	*,*,11	*,16,66
Aluminum (Al)	Trace Metals by ICP-MS	0.003	ppb (ug/l)	*	*	0.004	*
Antimony (Sb)	Trace Metals by ICP-MS	0.002	ppb (ug/l)	*	*	*	*
Arsenic (As)	Trace Metals by ICP-MS	0.005	ppb (ug/l)	*	*	*	*
Barium (Ba)	Trace Metals by ICP-MS	0.001	ppb (ug/l)	*	*	0.005	0.002
Beryllium (Be)	Trace Metals by ICP-MS	0.003	ppb (ug/l)	*	*	*	*
Bismuth (Bi)	Trace Metals by ICP-MS	0.001	ppb (ug/l)	*	*	*	*
Boron (B)	Trace Metals by ICP-MS	0.05	ppb (ug/l)	2.9	3.2	1.8	2.2
Cadmium (Cd)	Trace Metals by ICP-MS	0.003	ppb (ug/l)	*	*	*	*
Calcium (ca)	Trace Metals by ICP-MS	0.2	ppb (ug/l)	*	*	*	*
Cerium (Ce)	Trace Metals by ICP-MS	0.001	ppb (ug/l)	*	*	*	*
Cesium (Cs)	Trace Metals by ICP-MS	0.001	ppb (ug/l)	*	*	*	*
Chromium (Cr)	Trace Metals by ICP-MS	0.004	ppb (ug/l)	*	*	*	*
Cobalt (Co)	Trace Metals by ICP-MS	0.001	ppb (ug/l)	*	*	*	*
Copper (Cu)	Trace Metals by ICP-MS	0.003	ppb (ug/l)	*	*	*	*
Dysprosium (Dy)	Trace Metals by ICP-MS	0.001	ppb (ug/l)	*	*	*	*
Erbium (Er)	Trace Metals by ICP-MS	0.001	ppb (ug/l)	*	*	*	*
Europium (Eu)	Trace Metals by ICP-MS	0.001	ppb (ug/l)	*	*	*	*
Gadolinium (Gd)	Trace Metals by ICP-MS	0.001	ppb (ug/l)	*	*	*	*
Gallium (Ga)	Trace Metals by ICP-MS	0.002	ppb (ug/l)	*	*	*	*
Germanium (Ge)	Trace Metals by ICP-MS	0.003	ppb (ug/l)	*	*	*	*
Gold (Au)	Trace Metals by ICP-MS	0.006	ppb (ug/l)	*	*	*	*
Hafnium (Hf)	Trace Metals by ICP-MS	0.001	ppb (ug/l)	*	*	*	*
Holmium (Ho)	Trace Metals by ICP-MS	0.001	ppb (ug/l)	*	*	*	*
Indium (In)	Trace Metals by ICP-MS	0.001	ppb (ug/l)	*	*	*	*
Iridium (Ir)	Trace Metals by ICP-MS	0.002	ppb (ug/l)	*	*	*	*
Iron (Fe)	Trace Metals by ICP-MS	0.02	ppb (ug/l)	*	*	*	*
Lanthanum (La)	Trace Metals by ICP-MS	0.001	ppb (ug/l)	*	*	*	*
Lead (Pb)	Trace Metals by ICP-MS	0.003	ppb (ug/l)	*	*	*	*
Lithium (Li)	Trace Metals by ICP-MS	0.002	ppb (ug/l)	*	*	*	*
Lutetium (Lu)	Trace Metals by ICP-MS	0.001	ppb (ug/l)	*	*	*	*
Magnesium (Mg)	Trace Metals by ICP-MS	0.002	ppb (ug/l)	*	*	*	*
Manganese (Mn)	Trace Metals by ICP-MS	0.002	ppb (ug/l)	*	*	0.002	*
Mercury (Hg)	Trace Metals by ICP-MS	0.02	ppb (ug/l)	*	*	*	*
Molybdenum (Mo)	Trace Metals by ICP-MS	0.004	ppb (ug/l)	*	*	*	*
Neodymium (Nd)	Trace Metals by ICP-MS	0.001	ppb (ug/l)	*	*	*	*
Nickel (Ni)	Trace Metals by ICP-MS	0.004	ppb (ug/l)	*	*	*	*
Niobium (Nb)	Trace Metals by ICP-MS	0.001	ppb (ug/l)	*	*	*	*
Osmium (Os)	Trace Metals by ICP-MS	0.002	ppb (ug/l)	*	*	*	*
Palladium (Pd)	Trace Metals by ICP-MS	0.002	ppb (ug/l)	*	*	*	*
Platinum (Pt)	Trace Metals by ICP-MS	0.009	ppb (ug/l)	*	*	*	*
Potassium (K)	Trace Metals by ICP-MS	0.1	ppb (ug/l)	*	*	*	*
Praseodymium (Pr)	Trace Metals by ICP-MS	0.001	ppb (ug/l)	*	*	*	*
Rhenium (Re)	Trace Metals by ICP-MS	0.003	ppb (ug/l)	*	*	*	*
Rhodium (Rh)	Trace Metals by ICP-MS	0.001	ppb (ug/l)	*	*	*	*
Rubidium (Rb)	Trace Metals by ICP-MS	0.001	ppb (ug/l)	*	*	*	*
Ruthenium (Ru)	Trace Metals by ICP-MS	0.002	ppb (ug/l)	*	*	*	*
Samarium (Sm)	Trace Metals by ICP-MS	0.002	ppb (ug/l)	*	*	*	*
Scandium (Sc)	Trace Metals by ICP-MS	0.01	ppb (ug/l)	*	*	*	*
Selenium (Se)	Trace Metals by ICP-MS	0.02	ppb (ug/l)	*	*	*	*
Silicon (Si)	Trace Metals by ICP-MS	0.5	ppb (ug/l)	2.8	3.1	*	*
Silver (Ag)	Trace Metals by ICP-MS	0.001	ppb (ug/l)	*	*	*	*
Sodium (Na)	Trace Metals by ICP-MS	0.007	ppb (ug/l)	0.014	0.29	0.14	0.44
Strontium (Sr)	Trace Metals by ICP-MS	0.001	ppb (ug/l)	*	*	*	*
Tantalum (Ta)	Trace Metals by ICP-MS	0.004	ppb (ug/l)	*	*	*	*
Tellurium (Te)	Trace Metals by ICP-MS	0.004	ppb (ug/l)	*	*	*	*
Terbium (Tb)	Trace Metals by ICP-MS	0.001	ppb (ug/l)	*	*	*	*
Thallium (Th)	Trace Metals by ICP-MS	0.006	ppb (ug/l)	*	*	*	*
Thorium (Th)	Trace Metals by ICP-MS	0.003	ppb (ug/l)	*	*	*	*
Thulium (Tm)	Trace Metals by ICP-MS	0.001	ppb (ug/l)	*	*	*	*
Tin (Sn)	Trace Metals by ICP-MS	0.005	ppb (ug/l)	*	*	*	*
Titanium (Ti)	Trace Metals by ICP-MS	0.002	ppb (ug/l)	*	*	*	*
Tungsten (W)	Trace Metals by ICP-MS	0.005	ppb (ug/l)	*	*	*	*
Uranium (U)	Trace Metals by ICP-MS	0.002	ppb (ug/l)	*	*	*	*
Vanadium (V)	Trace Metals by ICP-MS	0.003	ppb (ug/l)	*	*	*	*
Ytterbium (Yb)	Trace Metals by ICP-MS	0.001	ppb (ug/l)	*	*	*	*
Yttrium (Y)	Trace Metals by ICP-MS	0.001	ppb (ug/l)	*	*	*	*
Zinc (Zn)	Trace Metals by ICP-MS	0.005	ppb (ug/l)	*	*	*	*
Zirconium (Zr)	Trace Metals by ICP-MS	0.005	ppb (ug/l)	*	*	*	*

Table 13. Leaching rate of Na and B based on results shown in Table 12.

1) Assume that Na is leaching from windows of all PMTs:

Parameter	Value on 12/13/1999	Unit
Na level (out-in)	0.276	ppb
SOB water volume	6	m ³
Water flow	18	m ³ /day
PMT window dia.	2.5	cm
Single PMT area	4.9	cm ²
Total PMT area	5.39	m ²
Leaching rate of Na+	0.004968	g/day
Leaching rate per pmt	4.51636E-07	g/(pmt*day)
Leaching rate of Na2O	6.08727E-07	g/(pmt*day)
Na2O content in glass	0.1338	g/cm ³
Leaching rate	4.54953E-06	cm ³ /(pmt*day)
Depth removal	9.28476E-07	cm/(pmt*day)
Depth removal	3.388936496	um/(pmt*yr)

2a) Assume that Boron is leaching from windows of all PMTs:

Parameter	Value on 12/13/1999	Unit
B level (out-in)	0.3	ppb
SOB water volume	6	m ³
Water flow	18	m ³ /day
PMT window dia.	2.5	cm
Single PMT area	4.9	cm ²
Total PMT area	5.39	m ²
Leaching rate of B+	0.0054	g/day
Leaching rate per pmt	4.90909E-07	g/(pmt*day)
Leaching rate of B2O3	1.66909E-06	g/(pmt*day)
B2O3 content in glass	0.3345	g/cm ³
Leaching rate	4.98981E-06	cm ³ /(pmt*day)
Depth removal	1.01833E-06	cm/(pmt*day)
Depth removal	3.716898092	um/(pmt*yr)

2b) Assume that Boron is leaching from only "frosty" PMTs:

Parameter	Value on 12/13/1999	Unit
B level (out-in)	0.3	ppb
SOB water volume	6	m ³
Water flow	18	m ³ /day
PMT window dia.	2.5	cm
Single PMT area	4.9	cm ²
Total PMT area	0.0245	m ²
Leaching rate of B+	0.0054	g/day
Leaching rate per pmt	0.000108	g/(pmt*day)
Leaching rate of B2O3	0.0003672	g/(pmt*day)
B2O3 content in glass	0.3345	g/cm ³
Leaching rate	0.001097758	cm ³ /(pmt*day)
Depth removal	0.000224032	cm/(pmt*day)
Depth removal	817.7175803	um/(pmt*yr)

Table 14. Various test results performed at SLAC, which correspond to the time when water samples were measured by Balazs Analytical Laboratory (this is addendum to Tables 12 & 13).

IR2 WATER QUALITY 1-st TEST RESULTS					
SLAC measurements of water transmission, pH factor, water resistivity and temperature ---->					
Parameter	Unit	Results		Results	
Date		12/13/99		8/21/00	
pH SUPPLY	PH Ffactor	6.7		6.5	
pH RETURN	PH factor	6.3		6.6	
R-water SUPPLY	Mohm.cm	13.4		18.5	
R-water RETURN	Mohm.cm	8.3		9.7	
T-water temp.	deg C	24.3		27.1	
Water flow	One volume change every	8 hours		24 hours	
Trans. (442nm)	%/meter	99.14	+ - 0.1	98.09	+ - 0.02
Trans. (325nm)	%/meter	98.56	+ - 0.7	98.05	+ - 1.7
Trans. (266nm)	%/meter	91.23	+ - 1.3	91.86	+ - 0.8
Comment		Old filters		New filters	
UV lamp		185 nm		260 nm	

Table 15. Water composition in Super Kamiokande (SK) and K2K experiments, which also use a pure water [15].

Parameter	Reference	K2K SUPP	K2K RETU	SK SUPPL	SK RETUR	SK 20 m	SK 37 m	Units
	3/21/99	3/21/99	3/21/99	3/21/99	3/21/99	3/21/99	3/21/99	
Aluminum (Al)	< 0.1	0.2	1.7	< 0.1	< 0.1	< 0.1	< 0.1	ppb (ug/l)
Calcium (ca)	0.23	0.073	2.4	0.11	0.82	0.29	0.29	ppb (ug/l)
Copper (Cu)	< 0.01	< 0.01	< 0.01	< 0.01	< 0.01	< 0.01	< 0.01	ppb (ug/l)
Iron (Fe)	< 0.01	0.04	0.26	< 0.01	0.03	0.03	< 0.01	ppb (ug/l)
Magnesium (Mg)	0.05	0.005	0.24	< 0.005	0.016	0.03	< 0.005	ppb (ug/l)
Sodium (Na)	0.054	0.28	0.13	0.34	0.29	0.3	0.36	ppb (ug/l)

Note: List only elements they have measured.

Table 16. Water parameters for K2K and Super Kamiokande (SK) experiments [15].

Parameter	K2K	S. K.
Date	3/21/99	3/21/99
pH SUPPLY	6	6
pH RETURN	6	6
R-water SUPPLY	16	18
R-water RETURN	9	10
T-water temp.	12	12
Water flow	2-3 day	2 month

5.7. Long-Term Test of PMT Front Glass Coupons in the SOB Water Return

We have decided to place twelve PMT front glass window coupons into the SOB vessel water return. The coupons were supplied by ETL as B53 glass, which is known to contain Zn. Neither Saclay nor SLAC obtained the X- glass coupons, and thus, we could not verify its corrosion rate independently of ETL. The coupons were placed into KYNAR holders (a special plastic resistant to water corrosion), as shown in Fig. 30. The holders were inserted in LEXAN container with a N₂ atmosphere above water. The container was placed in a thermally insulated housing, and the temperature was controlled at 30°C. This is close to SOB water temperature, which is 26-28°C. Therefore, no extrapolation is necessary. We report the results obtained after ~8 months of the coupons being immersed in water. We have confirmed this by running ESCA analysis – see Figure 32. One major result of the back scattered X-ray analysis, shown in Fig. 31, is that Na is almost completely depleted from the first few microns of the glass. This is also verified in the ESCA analysis shown in Fig. 32, which is sensitive up to the first ~50Å. The glass coupons appeared clear, as judged by visual inspection, when removed

from the water. However, we have observed crazing when the coupons were placed into vacuum during a surface analysis, as shown in Fig. 33. The crazing affected coupons independently, whether they were pumped on or not during the test, and was obvious by even naked eye. One could qualify it as “milky” rather than “frosty” surface from the point of view of our previous discussions. The flakes appear to be very shallow, and few microns thick. In other words, a PMT would operate normally, and with water coupling, we would not see any deterioration of efficiency. This result would be consistent with the ETL manufacturer’s finding that it is Zn, which prevents “frosting” development in this particular glass material. We still observe Na depletion and the front window turns “milky,” however, these corrosion effects are much smaller, and DIRC would operate well over the next ten years.

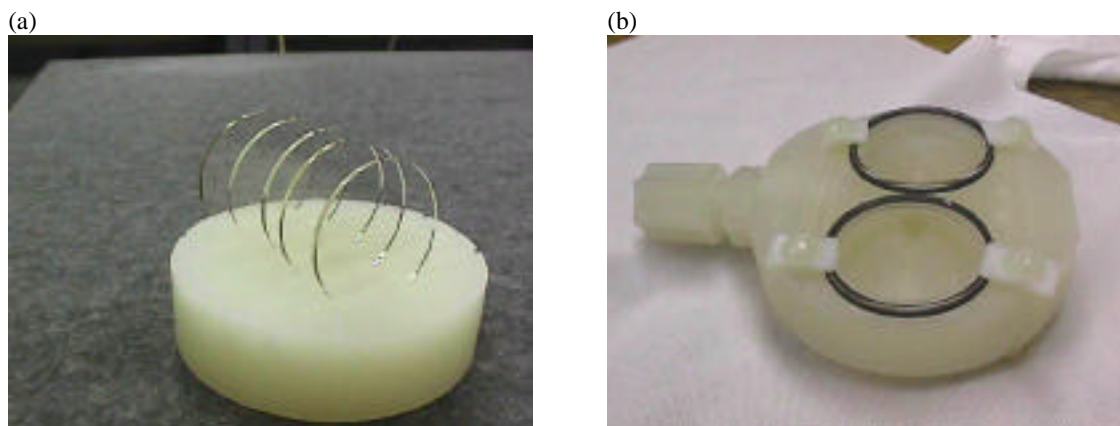


Figure 30. (a) A five-coupon setup placed in the SOB water return. (b) A two-coupon setup, which was pumped on.

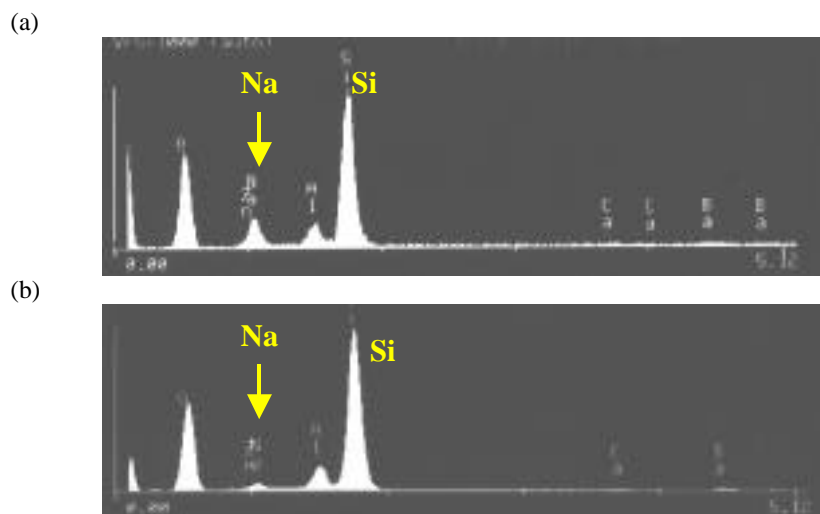


Figure 31. (a) X-ray analysis of the PMT front glass coupon A1 before the water test was started. The Na element is clearly detected. (b) The same coupon after eight months in the SOB water return. From the relative ratio of the Na/Si peak areas, it is clear that the Na line is depleted.

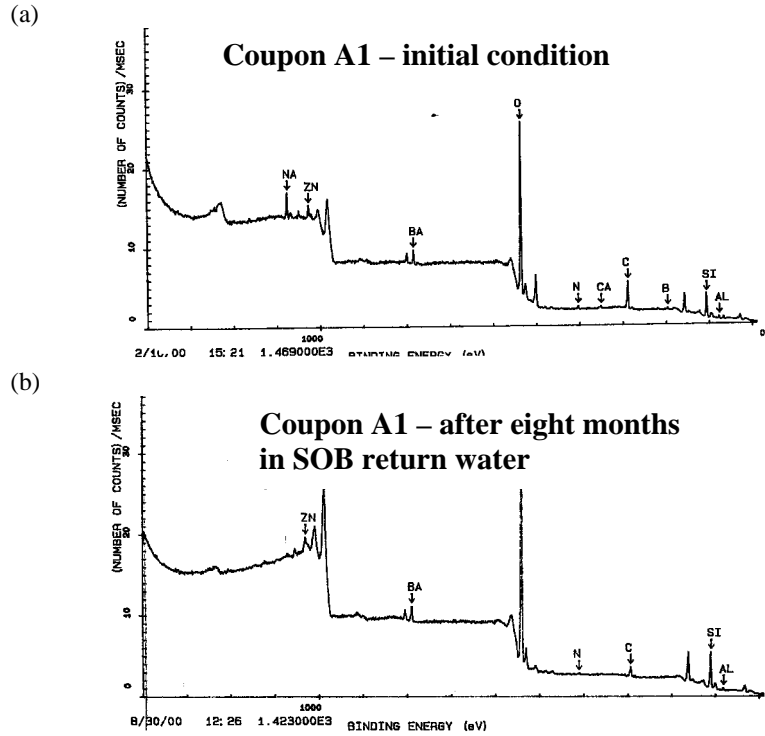


Figure 32. (a) ESCA analysis of PMT front glass coupon A1 prior to the water test. Both elements, Zn and Na, are clearly detected. This proves that this particular glass has traces of the Zn element present. (b) The same coupon after eight months in the SOB water return. The Na line is completely missing. The Zn line is still present.

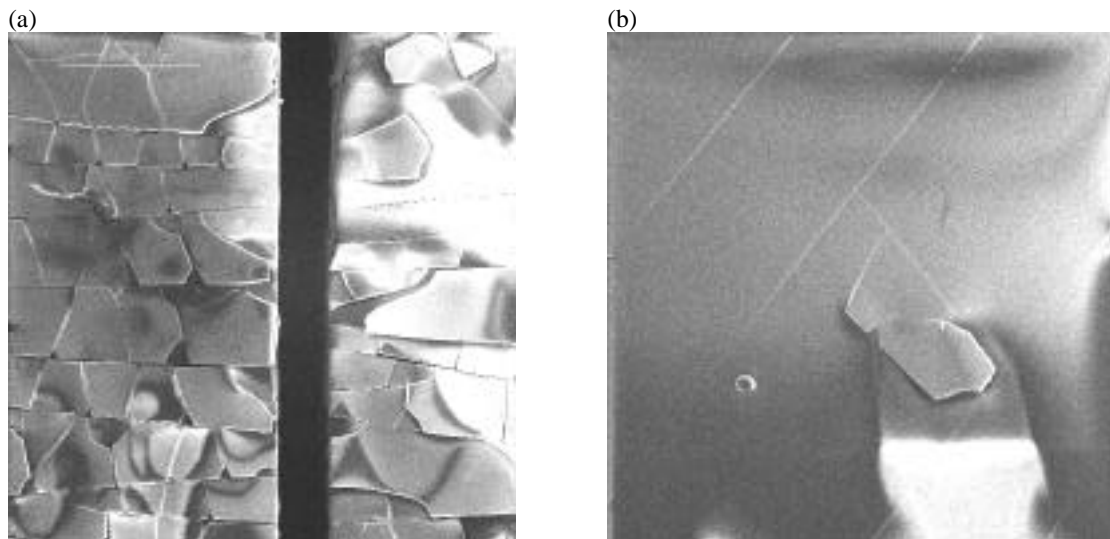


Figure 33. (a) Electron microscope picture of the PMT front glass coupon near the edges of C3 (left) and C5 (right) coupons. C5 coupon was subject to vacuum, C3 was not. They seem to be affected similarly. This type of surface gives a “milky” appearance as discussed elsewhere. (b) Similar picture of the middle C3 coupon, although, the corrosion level is generally lower. The “milky” appearance is spotty in the middle of the coupon.

5.8. Conclusion of Tests at SLAC

The SLAC analysis, using the electronic microscope, has determined that sodium depletion affects only the front window glass, for both “milky” and “frosty” PMTs. The PMT side glass is not affected.

Similarly, it was determined that using the ESCA analysis the “frosty” PMTs do not contain Zn, thus confirming the ETL result indicating the PMT material to be X-glass, which was added into production in error.

A long-term test of the B53 glass coupons, placed in SOB return water at 30°C, which is close to our operating temperature of 26-28°C in IR-2 (and therefore no scaling is required), shows corrosion to be consistent with that of the “milky” PMTs. The sodium is also depleted from the first few microns of surface. Such corrosion, although clearly visible if the glass is not coupled to water, will not represent a disaster for the DIRC from the point of view of possible PMT implosion.

Any time a “milky” PMT was subject to vacuum with the electron microscope, it developed additional crazing. This is a warning that the front PMT glass is very fragile, because of its depleted sodium. Therefore, the PMTs in the SOB must not be subjected to mechanical forces, which includes water draining or door opening.

A trace analysis of the water shows that the amount of sodium present in water is consistent with the sodium leaching from the front PMT glass, and represents a rate of removal of about 3-4 $\mu\text{m}/\text{PMT}/\text{year}$. This is consistent with the visual corrosion observed with the electron microscope on the “milky” PMTs.

The water analysis in DIRC is indicating a steady reduction of the bacteria level, which is a necessary condition to guarantee good transparency given the degree of glass corrosion.

The water analysis also indicates that DIRC does not have excessively pure water compared to experiments such K2K or Super Kamiokande.

6. Discussion

The purpose of this section is to point out that the “Zn hypothesis” may not be the “all explaining” recipe, and that the answer may lie in the detailed understanding of particular “glass” chemistry. For example, Table 17 shows that in the Pyrex type of glass, as used in Super Kamiokande, there is no Zn at all, and there is no corrosion of the PMT glass window [15]. Apparently, Zn is necessary in some Borosilicate glass formulations. Both ETL and us certainly did observe a very large corrosion of the X-glass window, which was added to DIRC PMT production in error (see Sections 1 and 2). If the correct B53 glass is used for the windows, the corrosion is much smaller (only a sodium depletion causing “milky” surfaces). However, we did not see any Na leaching and corrosion on the sides of the body glass of the DIRC PMTs [16], which is also a Borosilicate glass, and has no Zn nominally – see Table 17. Of course, the side glass comes as a tube and goes through a completely different process. Another example is the experience of Philips Photonics with the so called ZK(N)7 glass, which contained a very large amount of Zn (see Table 17), and an extremely large rate of corrosion was observed already in humid air [17].

Therefore, it appears that glass corrosion is dependent on a very delicate balance of various glass ingredients, and Zn may play a significant protection role only if present in the glass with the correct quantity. In case of the DIRC PMT, the front window glass requires a few percent of Zn in order to limit the corrosion rate, based on the empirical observations presented in this paper.

Based on our experience, we would always recommend that one perform as exhaustive a corrosion test as possible for particular choices of glass formulation.

Table 17. Comparison of PMT glass composition in various experiments or tests by the PMT manufacturers.

Company	Experiment	Glass name	PMT portion	SiO2	Al2O3	B2O3	Li2O	Na2O	K2O	BaO	CaO	As2O3	Sb2O3	ZnO
Hamamatsu	Super Kamiokande	Pyrex	face	80	2.1	14.1	0.1	3.7	0.12	-	-	-	-	-
Hamamatsu	Internal R&D test			-	-	-	-	5.5	-	-	-	-	-	-
Hamamatsu	Internal R&D test			67.5	3	19	0	0.4	9	-	-	-	-	-
Hamamatsu	Internal R&D test			65	0	14	0	0.1	0.06	-	-	-	-	-
Philips Photonics	A special PMT	ZK(N)7	face	60.8	5.6	14	-	7.4	0.003	-	-	0.1	0	11.2
Electron Tube Ltd.	DIRC detector	Borosilicate (B53)	face	65	6	15	-	6	-	3	1	-	-	4
Electron Tube Ltd.	DIRC detector	Borosilicate	side body	71	7	11	-	6	1	2	1	-	-	-
Electron Tube Ltd.	DIRC detector	Borosilicate	pin area	73	5	13	-	8	0.1	-	-	-	-	1
Electron Tube Ltd.	Internal PMT	X glass	window	69.6	4.2	17.2	-	8.7	-	0	0	-	-	0

7. Overall conclusion

We believe that the DIRC detector has about 50 “frosty” PMTs out of 11,000, where glass will be corroded to such an extent that over a 10-year period there may be a danger of implosion or vacuum loss. The ETL Co. explains that during the production a wrong type of glass was included, namely, so called X-glass, instead of B53 glass. The X-glass does not contain Zn, which, according to ETL, makes it weaker in terms of rapid leaching of sodium and boron resulting in the so-called “frosty” PMTs. We have provided independent experimental evidence in this paper supporting this hypothesis. The rest of the DIRC PMTs used B53 glass, which contains Zn, and this in turn limits the sodium and boron depletion to an acceptable level. There is still glass corrosion up to 30-50 μm of depth after ~ 10 years of operation, which is believed to be acceptable from the point of view of the danger of implosion.

DIRC’s data seems to indicate a non-negligible loss of detection efficiency at a level of 2-3% per year, both in Bhabha and di-muon events. Based on the Saclay test results, this loss could be explained by either window transmission or PMT quantum efficiency loss; however, the PMT gain loss cannot be excluded either. A simple estimate of the total PMT accumulated anode charge would favor the PMT gain loss explanation as a dominant factor. Of course, the small PMT gain change can be easily corrected by a corresponding change in voltage. More studies are needed to understand this in more detail.

Acknowledgment

We would like to thank R. Aleksan, V. Lepeltier, and G. Vasseur for their very valuable help in effort to understand the PMT glass corrosion problem. We also thank B. Kirby and his group at SLAC, for running the electron microscope and ESCA analysis spectrometer and provided many useful suggestions for the SLAC-based analysis. We thank A. Hoecker for his help in sorting out tube appearances during the October 1999 shutdown, and B. Ratcliff for suggesting using the water analysis results to check the consistency of the PMT corrosion rates. We also thank R. Reif for help to set up the long-term glass coupon test at SLAC.

References:

1. A. Hoecker, <http://www.slac.stanford.edu/~hoecker/IR2/frostyPMT.html>, October 1999.
2. J. Va’vra, BaBar *Hypernews note #595*, October 5, 1999.
3. Electron Tubes Limited, *Water immersion tests*, July 2000.
4. P. Bourgeois et al., BaBar *Hypernews note #993*, September 28, 2000.
5. J. Va’vra, BaBar *Hypernews note #764*, January 29, 2000.
6. The Saclay group, *PMT specifications and EMI 9125*, BaBar DIRC note 32, March 1996.
7. Ph.Bourgeois, M.Karolak and G.Vasseur, *Performance of the photomultiplier tubes used in the DIRC of BaBar: effect of a magnetic field and of helium*, Nucl.Inst.Meth. A442 (2000) 105.
8. P. Bourgeois et al., *Results of the PMT sector test at Saclay*, BaBar DIRC note 116, January 1999.
9. P. Bourgeois et al., *The light generator crate of the DIRC calibration system*, BaBar DIRC note 118, March 1999.
10. P. Bourgeois et al., *Results of the tests of the optical fibers and the diffuser for the DIRC calibration system*, BaBar DIRC note 119, March 1999.
11. T. Wright, ETL, private communication.
12. R. McAlpine, ETL technical Director, private communication.
13. A. Hoecker, http://www.slac.stanford.edu/~hoecker/plots/nphot_bhabha.gif.
14. D. Aston, BaBar *Hypernews note #986*, September 22, 2000.
15. S. Mine, K2K experiment, KEK, Japan, private communication.
16. J. Va’vra, BaBar *Hypernews note #700*, December 18, 1999.
17. Esso Flyckt, Photonis, private communication.